

# Sensors & Diagnostics

[rsc.li/sensors](https://rsc.li/sensors)



ISSN 2635-0998



Cite this: *Sens. Diagn.*, 2022, **1**, 312

## Paper-based sensors for diagnostics, human activity monitoring, food safety and environmental detection

Zhuoqi Yao,<sup>a</sup> Philip Coatsworth,<sup>b</sup> Xuewen Shi,<sup>a</sup> Jiacai Zhi,<sup>a</sup> Lixuan Hu,<sup>a</sup> Ren Yan,<sup>a</sup> Fırat Güder<sup>b</sup> and Hai-Dong Yu   <sup>\*a</sup>

Received 24th January 2022,  
Accepted 11th March 2022

DOI: 10.1039/d2sd00017b

rsc.li/sensors

Paper-based sensors exploiting the advantages of paper can replace traditional substrate materials for building sensors which are simple to manufacture, inexpensive, easy-to-operate, portable and disposable. From clinical diagnostics and agriculture to wearable devices and environmental and food science, paper-based sensors have enormous potential for applications, especially in resource-constrained settings. In this review, we summarize and discuss the latest research concerning paper-based sensors for applications in diagnostics, food, environment, agriculture and wearable sensing. We analyze the current challenges, offer potential solutions and highlight the opportunities.

### 1. Introduction

Sensors can detect and measure environmental information and subsequently transform the perceived information into electrical, optical and other quantifiable signals that can be digitized for processing, storage, transmission and display. In the era of the internet-of-everything, the demand for quick and efficient access to reliable information is increasing, which makes sensors even more important.<sup>1</sup> Inexpensive and easy-to-use sensors are key to obtaining information quickly and efficiently, realizing long-term real-time monitoring, and promoting the application of sensors in the world, especially in low-income areas. Paper-based sensors typically use paper substrates divided into different regions modified to be sensitive to a desired substance, and by creating specific fluid or gas channels, multiple detection regions can be used in parallel to improve the detection efficiency.<sup>2,3</sup> In addition to the ability to transform physical, chemical or biological changes in the environment into analytical signals, paper-based sensors are affordable, efficient and easy-to-use devices for fast or single-shot measurements, without the fear of contamination.<sup>4</sup> The application of paper-based devices can be traced back to semi-quantitative detection of glucose in urine in 1956.<sup>5</sup> Since then, detection devices such as pregnancy test paper have been developed further, and in

2007, George Whitesides and co-workers at Harvard developed a paper-based microfluidic device<sup>6</sup> which could detect both glucose and protein in simulated urine simultaneously. They proposed a micro-analysis device with printed microfluidic channels that did not require traditional materials<sup>2</sup> such as quartz, glass, silicon and polymers for the construction of the fluidic elements. Instead, paper-based microfluidics exploited the intrinsic characteristics of paper to wick water by capillary action.<sup>7,8</sup> Compared with substrate materials of other microfluidic detection platforms, paper also has advantages in cost, flexibility and passive fluidic transportation.<sup>9</sup> In addition, the various properties of paper, such as thickness, porosity, roughness and wettability, make it possible to precisely regulate the microfluidic behavior to meet various requirements.<sup>10</sup> For example, microfluidic channels can be prepared by printing, microfluidic flows can be regulated, and longitudinal fluid transport can be produced by folding three-dimensional devices. Paper is also a biopolymer and can be sustainably produced and degraded, making it unique among traditionally used petroleum-based plastic substrates. These many advantages of paper-based sensors have attracted great interest from researchers, and new explorations have been made, such as disease diagnosis, food safety sensing, environmental detection and human physiological monitoring.

Recently, research has focused on developing new classes of paper-based sensors with improved performance. Some of these recent sensors include all-paper piezoresistive sensors for human movement detection,<sup>11</sup> hydrophobic paper sensors with gas permeability for gas detection,<sup>12</sup> nano-cellulose paper sensors for multi-channel biological detection,<sup>13</sup> temperature sensors<sup>14</sup> and humidity sensors.<sup>15,16</sup> In addition

<sup>a</sup>Frontiers Science Center for Flexible Electronics, Xi'an Institute of Flexible Electronics (IFE) and Xi'an Institute of Biomedical Materials & Engineering, Northwestern Polytechnical University, 127 West Youyi Road, Xi'an 710072, PR China. E-mail: iamhdyu@nwpu.edu.cn

<sup>b</sup>Department of Bioengineering, Imperial College London, SW7 2AZ, UK



to sensors, paper has also been used for creating microfluidic batteries,<sup>17,18</sup> self-powered devices,<sup>19–22</sup> supercapacitors,<sup>23–25</sup> wet generators<sup>26</sup> and other types of paper-based devices.

In this review, we will walk you through a journey of how paper-based sensors are made and applied to solve challenging analytical problems. We will discuss recent research on paper-based sensors for medical diagnosis, food/environmental analysis, human behavior and physiological monitoring, and offer solutions to address the unmet needs and challenges involving paper-based sensors. Finally, we will share our outlook and forecast on future trends and insights into paper-based sensors, such as telemedicine and big data.

## 2. Paper as a substrate for sensors

Paper has been used for centuries in daily life, having an important impact on culture, economy and many other aspects of life.<sup>27,28</sup> With the increasing enrichment of raw materials and improvement of manufacturing processes, paper with different characteristics has been prepared for different applications, and many devices with specific functions have been developed using different types of paper as the base material.<sup>29,30</sup>

### 2.1 Preparation and structure of paper

Paper is made from raw materials containing plant fibers by pulping, blending, manufacturing and processing, and can be folded and cut at will.<sup>31,32</sup> In the pulping process, different fillers such as pigments and chemical additives are added to give paper different characteristics. During processing, sizing, calendering and drying are used for forming and dewatering, and finally the paper is given different appearances and sizes to achieve different application purposes.<sup>29</sup> For example, (i) adding mineral fillers such as calcium carbonate and clay to pulp can improve the light scattering, ink absorption and smoothness of paper; (ii) by adding pulp, such as starch, gum and rosin, the liquid absorption of paper can be reduced and the strength of paper can be improved; (iii) adding pigment coating and calendering to achieve a smooth surface and reduce pore size.<sup>28,33</sup>

Paper is a three-dimensional sheet formed by combining cellulose fibers of different lengths through hydrogen bonds between hydroxyl groups. The longer fibers give the paper good strength, while the shorter fibers fill the spaces between the longer fibers to reduce the pore size and make the paper

opaque. In addition, the cellulose fibers have a high aspect ratio, which leads to anisotropic properties.<sup>29</sup> Cellulose fibers somewhat determine the properties of paper, and so these properties can be adjusted by changing the length, diameter, and physical and chemical properties of the cellulose fibers used in production. For example, paper made from pulp obtained by mechanical treatment, known as wood-containing paper, becomes brittle and turns yellow gradually with the passage of time due to lignin.<sup>29</sup> In wood-free paper, paper produced by chemically treating pulp, the lignin is removed and more long cellulose fibers are produced to make the paper more porous.<sup>33</sup> With the continuous enrichment of paper types, the many uses of paper only increase, and common everyday uses include writing, painting, printing, packaging and wiping. The appearance of paper has made an indelible contribution to the development of history and the spread of culture.

### 2.2 Advantages of paper as a sensor substrate

Low-income regions of the world generally cannot offer extensive medical services at a low cost. Standard medical tests performed in centralized laboratories are either nonexistent or prohibitively expensive for most citizens in developing countries. It is, therefore, necessary to develop fast, efficient, easy-to-operate, and inexpensive detection devices that can be used in resource-limited settings. As a substrate, compared with traditional sensor substrates, paper has the characteristics shown in Table 1, making it ideally suited for the fabrication of low-cost lab-on-a-chip type diagnostics.<sup>34–36</sup>

Paper-based detection platforms are not only widely used in the scientific community, but also have great development potential in everyday life, even in places with limited resources, such as remote areas and during emergency situations.<sup>37,38</sup> Paper-based flexible electronics have made rapid development due not only to paper-based microfluidics, but also due to progress in paper-based mechanical sensing, humidity sensing and self-energy supply.

### 2.3 Different types of paper

Filter paper is the most widely used paper type in paper-based microfluidic sensors.<sup>39,40</sup> Being composed of pure cellulose, filter paper contains only the intrinsic impurities originating from the fiber.<sup>2</sup> Whatman #1 produced by General Electric Healthcare is currently the most popular

**Table 1** Nature of paper

Nature	Result
Flexibility	The three-dimensional structures can be formed by folding
Thickness	The small thickness allows relatively few reagents to be used in device fabrication
Adsorption	A volume of reagent can be stored and transported in the paper matrix
Large specific surface area	The number of immobilized enzyme molecules and colorimetric probes increased
Capillary action	Capillary forces can be used to transport liquids in all directions without the need for a pump
Biodegradability	It can be biodegraded by microorganisms or incineration to prevent biological hazards



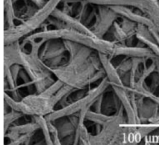
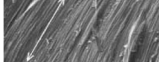
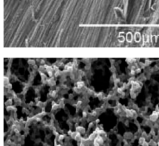
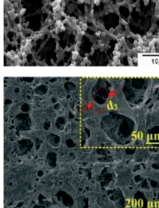
brand of paper used in the fabrication of paper-based sensors, having a smooth surface, uniform texture, moderate flow rate and 0.18 mm thickness. Whatman #1 is also suitable for printing and hence compatible with high-volume manufacturing.<sup>41</sup> Although filter paper is widely used, it does not always have the required physical properties, and so other types of paper or paper modification methods have been explored. The microstructure of filter paper and some newly developed cellulose papers with special properties is shown in Table 2. These cellulose papers have a different microstructure, leading to their unique properties and enabling the development of new paper-based devices.

Nitrocellulose paper has been widely utilized in the paper-based sensor field due to its advantages of easy binding of proteins with high efficiency.<sup>42</sup> Lu *et al.*<sup>43</sup> studied the preparation of paper-based sensors using nitrocellulose films as substrates. A wax barrier was first formed on the film by printing and heating, and the enzyme was then deposited for colorimetric determination. Although the nitrocellulose membrane was smooth and uniform in pore size, making the flow of the liquid in the paper more stable and repeatable, the seepage velocity of wax on the nitrocellulose membrane was slower than that on filter paper. Jiang *et al.*<sup>44</sup> studied the preparation of paper-based microfluidic detection devices in combination with nitrocellulose film, glass-cellulose film and

filter paper for the detection of bladder cancer. This device combined the protein immobilized by nitrocellulose film and the excellent water absorption property of filter paper to ensure the dynamic flow of samples.

As a new form of paper, transparent paper has been widely studied in recent years. Different from traditional paper, transparent paper has high optical transparency and superior mechanical properties, and is an ideal substrate for new paper-based devices.<sup>45–48</sup> Zhong *et al.*<sup>49</sup> demonstrated a transparent paper-based self-supplying intelligent interactive system based on the electrostatic induction mechanism. The self-powered system can be used as an art anti-theft system due to the high transparency, so as to protect artistic works without affecting the appreciation. Zong *et al.*<sup>27</sup> designed a transparent paper-based chemical sensing platform for low-cost and highly sensitive detection of multi-target analytes by wavelength-dependent absorbance/transmittance. This chemical sensor based on transparent paper has been successfully applied to the detection of bovine serum albumin and serum cholesterol with detection limits of 0.1  $\mu$ M and 0.1 mM, respectively. Ying *et al.*<sup>50</sup> used nanofibrillated cellulose (NFC) paper as the base material to prepare transparent, pump-free and hollow channel paper-based microfluidic analytical devices. This device was used to detect glucose by colorimetry with a detection limit of 1.4

**Table 2** Microstructure and characteristics of some cellulose paper

Paper type	SEM images or photograph	Remarks	Typical paper devices
Whatman #1 filter paper		Almost consists of pure cellulose; no other impurities; superior aperture; the thickness is relatively uniform <sup>39,54</sup>	3D vertical flow paper-based device <sup>55</sup>
Nanocellulose paper. Adapted with permission from ref. 56. Copyright © 2016 American Chemical Society	 	Dense structure; glaze surface; high grade of transparency; good hydrophobicity <sup>11,56,57</sup>	All paper-based flexible and wearable piezoresistive pressure sensor. <sup>11</sup> Transparent paper-based device for multi-channel bioassay <sup>13</sup>
Inside the anisotropic transparent film showing aligned microfibers. Adapted with permission from ref. 58. Copyright 2021, Wiley-VCH		Anisotropy; high transparency; high mechanical tensile strength <sup>58</sup>	Electronic and fluid devices such as anisotropic mass transfer trigger circuit based on MoS <sub>2</sub> (ref. 58)
Nitrocellulose film. Adapted with permission from ref. 59. Copyright 2019 Elsevier B.V.		Excellent biocompatibility; unique physical and chemical properties; the ability to immobilize various biomolecules <sup>44,59</sup>	Paper-based microfluidic analytical device for bladder cancer diagnosis <sup>44</sup>
Transparent microcrystalline cellulose/polyvinyl alcohol paper. Adapted with permission from ref. 60. Copyright © 2020 American Chemical Society		Adjustable aperture; high light transmittance (>95%); good mechanical properties; excellent biocompatibility <sup>60</sup>	2D and 3D cell culture platforms <sup>60</sup>



mM. In addition, due to the high transparency of NFC paper-based devices, the authors also demonstrated SERS-based photochemical detection. Optical detection of rhodamine-B was demonstrated with a detection limit of 0.8  $\mu$ M. Transparent paper has been extensively studied due to its non-toxicity and biodegradability and can replace traditional paper or even plastic substrates in green sensor devices.<sup>51</sup>

At present, the modification of paper or other materials is another direction to which paper-based materials are heading. For example, hydrophobic paper has been applied to the substrate of an electrochemical detection device,<sup>52</sup> and paper has been combined with nanomaterials to improve the detection sensitivity of microfluidic devices.<sup>53</sup>

### 3. Fabrication methods

Mature device fabrication technology is a prerequisite for a wide range of sensor applications. Examining the wide range

of existing preparation techniques can help researchers to further improve on the existing basis and also help to select the appropriate preparation techniques during device production and preparation.

#### 3.1 Fabrication of 2D paper-based devices and electrodes

At present, the main research on paper-based sensors is focused on paper-based microfluidics. Therefore, this paper will focus on the preparation technology used for the construction of paper-based microfluidic channels (Fig. 1A).<sup>2,61</sup> These preparation methods can be divided into wax printing, lithography, inkjet printing, screen printing, plasma processing, mechanical cutting, manual pattern drawing and other methods according to the different construction methods and principles of micro-channels on paper. Two-dimensional paper-based microfluidic device construction begins with the formation of a hydrophobic

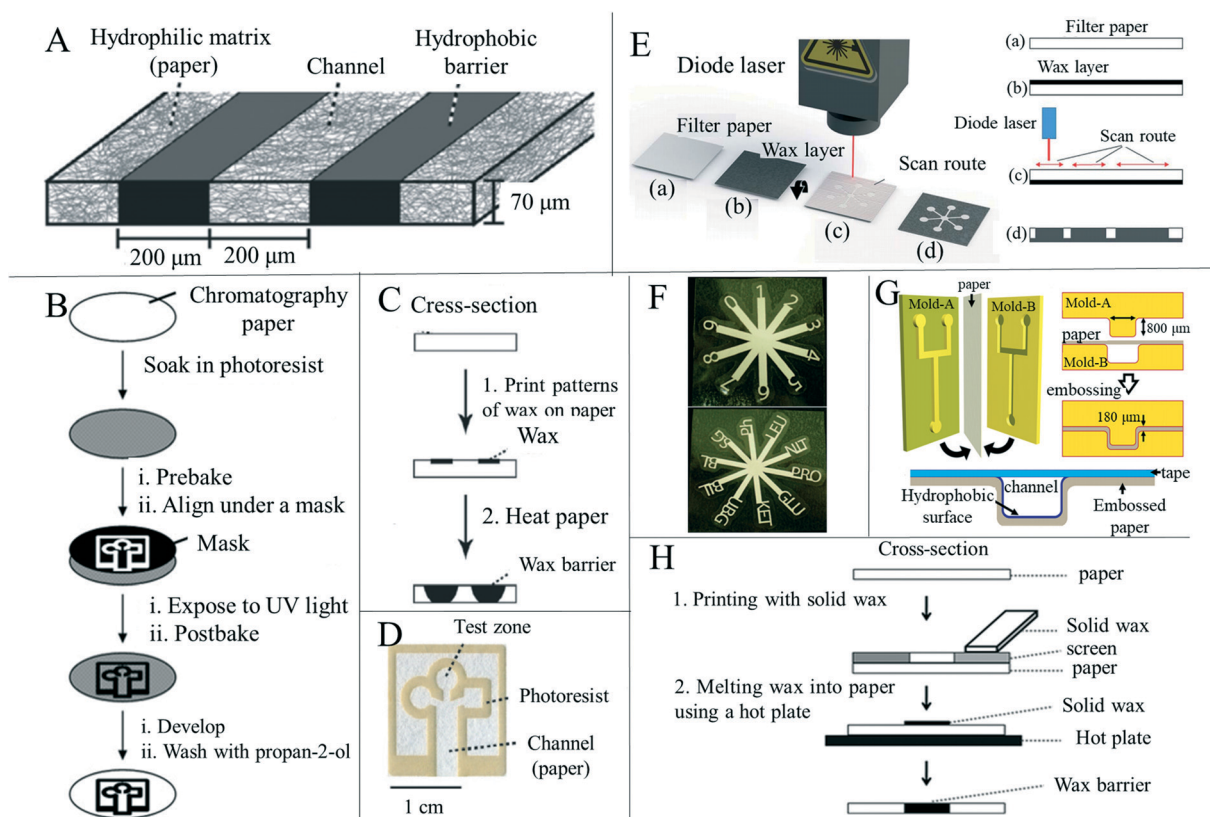


**Fig. 1** Techniques for processing the shape and structure of paper-based sensors. (A) Schematic diagram of the construction of paper-based microfluidic channels. Reproduced with permission from ref. 2. Copyright 2009, American Chemical Society. (B) Constructing a microfluidic channel using photolithography on a paper substrate. Reproduced with permission from ref. 6. Copyright 2007, Wiley-VCH. (C) Wax printing is used to construct microfluidic channels on paper. Reproduced with permission from ref. 2. Copyright 2009, American Chemical Society. (D) A paper-based microfluidic device was prepared by photolithography. The device delivered liquid to three partitions through the main channel. Reproduced with permission from ref. 2. Copyright 2009, American Chemical Society. (E) Laser scanning is used to produce paper-based microfluidics: (a) blank filter paper; (b) coated with an evenly distributed layer of wax; (c) laser scanning on the back of the paper; (d) the wax penetrates the entire thickness of the filter paper. Reproduced with permission from ref. 77. Copyright 2019, Royal Society of Chemistry. (F) Computer controlled X-Y knife plotter to construct patterns on the paper base. Reproduced with permission from ref. 76. Copyright © 2008 American Chemical Society. (G) Laminar flow in the open channel microfluidic device constructed by embossing the channel on Whatman#1 filter paper. Reproduced with permission from ref. 78. Copyright 2014, American Chemical Society. (H) Using wax as a hydrophobic material and screen printing technology to prepare paper-based microfluidic devices (schematic diagram). Reproduced with permission from ref. 70. Copyright 2011, Royal Society of Chemistry.



barrier on the paper by means of physical deposition or chemical modification, so as to form a channel conducive to microfluidic flow.<sup>62</sup> Subsequent further modification is then performed to achieve a paper-based sensor with a specific function. Based on the excellent properties of paper such as the three-dimensional porous fiber structure and moisture absorption characteristics, a variety of devices such as mechanical sensing, humidity sensing and gas sensing devices have been developed. The sensing layer of these devices is typically prepared by cutting, soaking and stacking. During device usage, electrodes are required to output changes in electrical signals caused by sensing, and so the preparation of electrodes during device development is also critical, where current preparation methods mainly include screen printing, ink-jet printing and drawing.<sup>63–65</sup> On the basis of meeting the requirements of low-cost, simple and efficient production, different manufacturing methods adjust the properties or shape of the paper by chemical modification, physical deposition and mechanical cutting, so that it can be further modified or directly applied to a series of applications.<sup>7</sup> In this paper, these methods are discussed, and the advantages and disadvantages of some preparation methods are compared and summarized (Table 3).

**3.1.1 Wax printing.** Wax printing involves using computer software to design the required pattern, printing the design with a wax printer onto the paper surface and melting the wax so it penetrates the entire depth of the paper substrate, often using a hot plate, oven or heat press.<sup>79,80</sup> Hydrophobic wax walls can be used in paper to form channels for fluid flow and setting areas for samples, storage and detection, according to need. Wax printing is generally considered to be the most popular method for creating hydrophobic barriers because of its relatively low cost, simple and fast printing process, and ability to create flexible patterns.<sup>9</sup> During the

wax printing process, printing the pattern on the paper and melting the wax into the paper to form a complete hydrophobic barrier are two key steps with considerations that should be taken into account (Fig. 1C). When wax is printed on paper and heated, the horizontal diffusion of wax on the paper reduces the resolution of the printed pattern, resulting in a hydrophobic barrier wider than the original printed pattern.<sup>63,67</sup> Improvements to the resolution of patterns printed in wax are being developed constantly. For example, Strong *et al.*<sup>81</sup> prepared microfluidic channels on paper by wax printing, followed by processing with periodate to obtain high-fidelity and high-resolution microfluidic devices. This new wax-based manufacturing method controls the size of the final microfluidic channel by varying the concentration of iodate and the reaction cycle, and also has certain prospects in applications for other devices. Wax printing has the advantages of being inexpensive, efficient, fast, and easy to manufacture in large quantities when preparing paper-based microfluidic equipment. Prototyping of microfluidic devices can be complete within five minutes, and small changes post-prototype can be achieved in even less time.<sup>67</sup> These advantages alongside only a small amount of equipment knowledge in the production process required suggest that the wax printing preparation technology will become an ideal method for microfluidic equipment mass production.

However, one problem that must be faced is that wax printers have been discontinued by manufacturers.<sup>82</sup> In addition to the preparation of paper-based microfluidic devices using wax printers retained in the laboratory, researchers are constantly exploring alternative ways to prepare paper-based microfluidic devices using wax as a hydrophobic material. Chiang *et al.*<sup>83</sup> demonstrated an alternative manufacturing method for single-step fabrication

**Table 3** Comparison of different paper-based microfluidic preparation technologies

Fabrication methods	Equipment	Principle	Advantages	Limitations
Wax printing <sup>66,67</sup>	Wax printer, hot plate	Hydrophobic compounds are physically deposited on the fiber surface	Simple, fast, and conducive to large-scale manufacturing	Low resolution and heating required
Photolithography <sup>2,6,68</sup>	Lithography machine, ultraviolet lamp, hot plate	Form a physical partition gap	High resolution and sharp microfluidic channels	Expensive equipment, complicated steps, expensive reagents
Screen printing <sup>69–71</sup>	Screen printing machine, customized mold	Hydrophobic compounds are physically deposited on the fiber surface	Low cost and simple operation	Low resolution, rough microfluidic channel walls, different molds need to be customized according to needs, not conducive to mass production
Inkjet printing <sup>72</sup>	Inkjet printers	Fiber surface chemical modification	High resolution, one device can meet the requirements	Depending on the equipment prepared, different inks are needed, the printer needs to be improved, and heating is required
Plasma treatment <sup>73–75</sup>	Plasma reactor, hot plate, custom mold	Fiber surface chemical modification	Use of cheap plate-making agent, low material cost	Need to customize the mold according to needs
Knife plotting <sup>76</sup>	X-Y knife plotter	Physical hydrophobic barriers are constructed by cutting	No hydrophobic modification materials are required	Possibility of tearing paper during cutting



of paper-based microfluidic devices using wax based on a 3D printing process. 3D printers have heating elements that allow wax to be distributed in liquid form, thus wax patterns can be printed on paper and solidified to form a hydrophobic barrier without the need for additional heating processes. As wax printing is a promising method for preparing paper-based microfluidic devices, we believe that the popularity of paper-based microfluidic devices and their commercial value will encourage more manufacturers to re-manufacture wax printers.<sup>84</sup>

**3.1.2 Screen printing.** Screen printing is performed by pushing ink, wax and other pastes through a mesh screen using a squeegee, where the ink is printed onto the substrate according to a pattern formed on the mesh with an impermeable stencil.<sup>70</sup> Hydrophobic substances such as ink and wax can be used to build hydrophobic barriers in paper and form microfluidic flow channels. Dungchai *et al.*<sup>70</sup> manufactured paper-based microfluidic devices by wax screen printing using two simple steps: printing a solid wax pattern on the surface of the paper with a simple screen printing method followed by melting the wax into paper with a hot plate to form a complete hydrophobic barrier (Fig. 1H). Jarujamrus *et al.*<sup>71</sup> used a rubber solution as a hydrophobic substance and screen printed it on the paper to form a hydrophobic barrier. The screen printing method can also be used to print the designed electrode pattern on paper, allowing for fast production speed, low cost and simplicity.<sup>79,85</sup> Cinti *et al.*<sup>85</sup> screen printed electrodes on a paper substrate and successfully prepared a paper-based electrochemical phosphate detection sensor. Caratelli *et al.*<sup>86</sup> prepared a three-electrode system for the electrochemical detection of cholinesterase inhibitors by manual screen printing. Screen printing is a relatively mature preparation method, the equipment and products used are relatively easy to obtain and the price is typically low, therefore it is an appropriate method for mass production and for producing small numbers of specially customized paper-based devices.

**3.1.3 Photolithography.** Paper-based microfluidic devices can be prepared by photolithography, where photoetching of a resist printed on the paper according to the design pattern forms a microfluidic channel composed of hydrophobic lines or walls, where fluid can flow in these channels depending on the capillary action of the paper.<sup>2</sup> Martinez *et al.*<sup>6</sup> constructed a hydrophobic barrier on a piece of paper by photolithography and extended it to the thickness of the whole paper (Fig. 1B). The authors impregnated the entire paper with photoresist (SU-8, SC) and exposed it to ultraviolet light through a transparent mask, with areas printed with black ink, to selectively polymerize the photoresist agent. The unexposed photoresist was then removed from the paper by washing (Fig. 1B).

**3.1.4 Plasma treatment.** The paper surface can be modified by plasma treatment to form a microfluidic channel. In 2008, Li *et al.*<sup>75</sup> reported a method for constructing a paper-based microfluidic channel using plasma treatment. Firstly, the paper base was treated with an

alkyl copper dimer. The treated hydrophobic paper was placed between metal masks with a design pattern and plasma treatment was performed to form a hydrophilic channel.<sup>75</sup> When plasma is used for hydrophilic channel construction, metal molds need to be customized, and different patterns are customized as required, leading to high costs, making this process unsuitable for mass production of paper-based microfluidic devices.

**3.1.5 Laser treatment.** Laser treatments use a variety of methods such as cutting and hot melting, and a laser is utilized to remove hydrophilic paper along the design structure, thereby creating a hydrophobic barrier at the edge of the cutting line.<sup>87</sup> Mahmud *et al.*<sup>87</sup> created a microfluidic channel on paper backed with aluminum foil, using a 30 watt CO<sub>2</sub> laser to cut the paper without the aluminum foil being penetrated. Another laser-based method involves heating the paper pre-coated with hydrophobic substances so that hydrophobic substances can penetrate at high temperature to form a hydrophobic barrier. Zhang *et al.*<sup>77</sup> deposited wax evenly on the paper surface, and used laser heating to make wax penetrate the paper to form hydrophobic barriers and microfluidic channels; the specific preparation process is shown in Fig. 1E. Laser techniques have also been used to remove specific areas of the hydrophobic material from the paper to create hydrophobic channels. Hiep *et al.*<sup>88</sup> used octadecyltrichlorosilane to hydrophobically treat the cellulose chromatography paper and then soaked a photoacid generator (CPI-410 s) into the paper, irradiating it with a 405 nm laser beam to trigger an acid producing reaction, thus forming a hydrophilic pattern in the light area. The bond between cellulose and octyl trichlorosilane was broken by the hydrolysis reaction and therefore the light irradiation area will become hydrophilic. This method can successfully create arbitrary hydrophilic patterns with a resolution of 50 μm.

**3.1.6 Mechanical processing.** Machining is the process of cutting or embossing the paper in accordance with the desired pattern, in order to build the channel needed for fluid flow. In mechanical processing, patterns are designed by a computer and cut or embossed according to the patterns by mechanical processing machines, and patterns formed by machining are often of high precision. In addition, the preparation of microfluidic devices has also been done through manual processing, convenient for experimental operation, although the accuracy of the devices is often inferior to those formed by automatic mechanical processing. Thuo *et al.*<sup>78</sup> used a computer designed mold, 3D printed from the acrylonitrile-butadiene-styrene copolymer, to manufacture an open-channel microfluidic device by sandwiching a piece of paper between two molds with complementary shapes (Fig. 1G). Kugimiya *et al.*<sup>89</sup> first used adhesive to attach a piece of filter paper to the carrier piece, then used a cutting plotter to cut according to the pattern designed by the software, removing unwanted edges and obtaining a strip of preset shape. Fenton *et al.*<sup>76</sup> constructed a physical hydrophobic barrier on a paper base by using a



computer-controlled X-Y knife plotter (Fig. 1F). By cutting, the unwanted material can be removed and a physical hydrophobic barrier of the desired pattern can be constructed on the paper base. This new method is suitable for device manufacturing and application in resource-poor areas, is suitable for both prototype development and high-volume manufacturing, and has improved the rates of operator error. In addition, cover film and laminating machines can be used to mass produce strips with specific shapes.

**3.1.7 Pyrolysis treatment.** Pyrolysis is another method to treat paper at present. After pyrolysis, paper retains the fiber structure and has a large specific surface area and low resistivity.<sup>90</sup> Pyrolytic paper is often used as an electrode material to construct paper-based sensors. Duran *et al.*<sup>91</sup> realized a one-step synthesis of copper nanoparticles (CuNPs) and their integration into paper-based carbon electrodes. Rich CuNPs were formed on the surface of carbonized cellulose fiber by pyrolysis of paper tape and modification by a saturated CuSO<sub>4</sub> solution. The pyrolyzed paper containing abundant CuNPs was used as the working electrode for non-enzymatic amperometric determination of glucose. The test results show a high linear response (up to 3 mM) and a high sensitivity ( $460 \pm 8 \mu\text{A cm}^{-2} \text{ mM}^{-1}$ ). Araujo *et al.*<sup>92</sup> used a single-step laser scribing process to draw electrodes with high conductivity and an enhanced active/geometric area ratio on paper-based devices. The electrode is a conductive porous non-graphitized carbon material consisting of a graphene sheet and an aluminosilicate nanoparticle composite material produced by carbon dioxide laser pyrolysis of the surface of a paperboard. This system was used to detect ascorbic acid and caffeic acid, demonstrating its application value. Nicoliche *et al.*<sup>93</sup> used pyrolytic paper as a porous electrode and cast off-the-shelf polysorbate on the electrode for coupling *in situ* to form hydrophilic nanocoating. The electrode utilizes the three-dimensional structure of pyrolytic paper to increase the detection area, and the hydrophilic layer on the surface prevents biological contamination. By means of functional nanomaterials modified on this electrode, the detection of SARS-CoV-2 was achieved. Shimizu *et al.*<sup>94</sup> achieved sensitive detection of phosphate using pyrolytic paper modified with isopropyl alcohol as a porous electrode. This pyrolytic paper can be produced in large quantities and can create independent structures in one cutting operation using a commercial knife plotter, demonstrating that pyrolytic paper is a promising alternative to standard electrodes. Pyrolytic paper has excellent electrical properties, but can be very fragile and easy to crack. In view of this, Damasceno *et al.*<sup>95</sup> reported an effective method to prepare flexible, foldable, twistable and stretchable electrodes from pyrolytic paper. The delayed capillary flow of elastomer was used to ensure that the pyrolytic paper had extremely high mechanical stability and electrochemical performance. Based on this stretchable electrode, a flexible and stretchable electrochemical device based on paper is possible.

**3.1.8 Other fabrication methods.** For the production of two-dimensional paper-based devices, other methods include drawing,<sup>14</sup> manual production and flexible printing.<sup>96</sup> Reynoso *et al.*<sup>97</sup> filled an empty ball pen with a solution of trichlorosilane and used the pen to draw lines on Whatman chromatography paper no.1 to construct a fluid channel. Trichlorosilane reacted with the paper to form a hydrophobic barrier. A glucose colorimetric test and enzyme-linked immunosorbent assay (ELISA) were performed to verify the repeatability of the preparation process and the applicability of the preparation device. Similarly, Ghaderinezhad *et al.*<sup>98</sup> used a desktop pen plotter to construct hydrophobic barriers on paper. This mode of operation is relatively simple, does not require expensive equipment and the patterns produced have high accuracy and repeatability, providing a new, simple and inexpensive method for the preparation of paper-based microfluidic devices. Ponram *et al.*<sup>99</sup> printed phosphorescent iridium(III) on composite paper by inkjet printing for the highly selective detection of Hg<sup>2+</sup>. Ng *et al.*<sup>82</sup> proposed a method for manufacturing a microfluid-based analytical device using toner laser printers. In this method, the paper on which the pattern is to be printed is heated to 200 °C so that the toner penetrates the paper to form a hydrophobic barrier.

Besides the screen printing and pyrolysis mentioned above, researchers have also tried other ways to prepare electrodes from conductive inks. Gaspar *et al.*<sup>100</sup> prepared a silver staggered electrode structure on a paper substrate by ink-jet printing and used paper itself as a sensing material to form a humidity sensor. Sundriyal *et al.*<sup>101</sup> prepared electrodes on an A4 paper substrate by inkjet printing to form a solid asymmetric supercapacitor. Hand painting is also a frequently used electrode preparation method. Liu *et al.*<sup>102</sup> drew conductive traces with high conductivity, remarkable foldability and stability on paper by using prepared ink and a ballpoint pen, and verified the performance of the electrode. This method can be used to quickly prepare electrodes without large-scale equipment, but major disadvantages include the influence of the painter, low repeatability and the inability to draw on a large scale. A mechanical plotter may help solve these issues; traces are drawn by computer design and a mechanical arm is used to control a pen containing ink, ensuring the consistency of electrode patterns and making batch preparation possible.

### 3.2 Fabrication of 3D paper-based devices

In recent years, scientists have expanded the research on paper-based sensors from two-dimensional (2D) to three-dimensional (3D) paper-based sensing devices, along with various preparation methods. Compared with 2D sensors, 3D paper-based sensors can perform more complicated and multichannel analysis in microfluid detection applications (Fig. 2A). At the same time, the longitudinal flow of fluid in the device requires fewer samples and less flow time than the transverse flow, thus enabling faster and more efficient detection and analysis. At present, the preparation method of 3D paper-based devices is mainly to stack individual 2D devices through various means



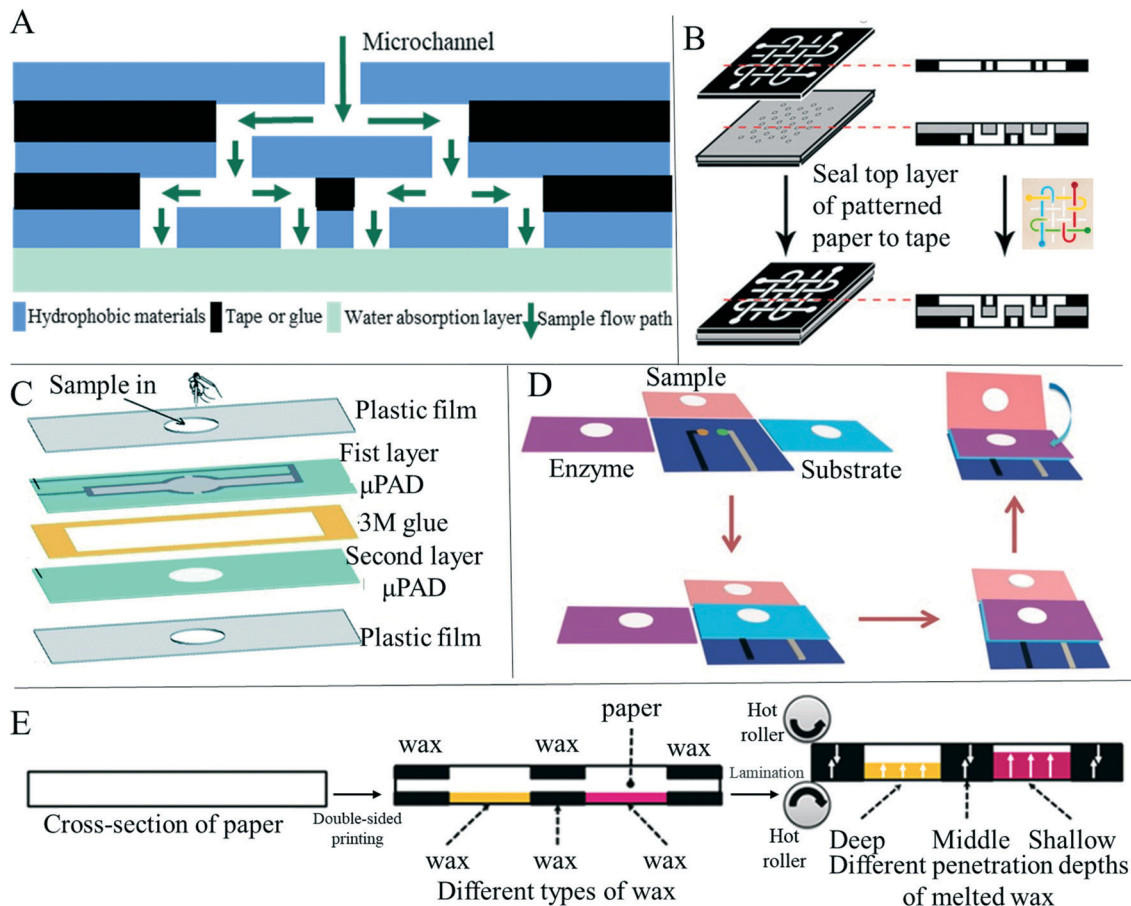


**Fig. 2** Preparation methods of 3D paper-based sensors. (A) Schematic diagram of microfluidic channels inside paper-based 3D devices. (B) Three-dimensional paper-based analytical devices with complex microchannels were prepared by adhesive tape bonding, which made them have stronger analytical ability. Reproduced with permission from ref. 104. Copyright 2008, National Academy of Sciences. (C) Two-dimensional paper layers with microfluidic channels prepared by wax printing are bonded by glue, forming devices with three-dimensional structures. Reproduced with permission from ref. 79. Copyright 2020, Royal Society of Chemistry. (D) Multi-channel paper-based electrochemical analysis devices were fabricated by folding. Reproduced with permission from ref. 106. Copyright 2016 Wiley-VCH Verlag GmbH & Co. KGaA, Weinheim. (E) Schematic diagram of the 3D microfluidic design and printing strategy based on single-layer paper. Reproduced with permission from ref. 110. 2021 Elsevier B.V. all rights reserved.

such as adhesive tape adhesion and folding.<sup>103</sup> Martinez *et al.*<sup>104</sup> introduced a method to fabricate 3D microfluidic devices using patterned paper and double-sided tape (Fig. 2B). The 3D paper-based equipment distributed the fluids vertically and horizontally, so that the fluids could cross each other without mixing, and then distributed the samples from a single-entry point to the detection area, which achieved simultaneous and efficient detection. Similarly, Wang *et al.*<sup>105</sup> used double-sided adhesive tape and wax printing to prepare a 3D paper-based sensor that could detect multiple heavy metal ions simultaneously. Guan *et al.*<sup>79</sup> prepared a 3D paper-based analysis device by means of glue adhesion, and set different functions on each layer, so that a single device acted as a multi-functional platform for plasma separation and fibrinogen detection of blood (Fig. 2C). However, preparing 3D paper-based devices using double-sided adhesive tape has some drawbacks, such as complex alignment, bonding, and punching processes, which can adversely affect fluid flow.<sup>9</sup> In addition, some researchers used origami to make three-dimensional

paper-based equipment to achieve simultaneous shunting and multiple testing. Ding *et al.*<sup>106</sup> designed a three-dimensional paper-based device constructed by folding (Fig. 2D). The device can be used for a general potential bioassay by folding and unfolding the structure of the paper. Teengam *et al.*<sup>107</sup> prepared a three-dimensional paper-based microfluidic device with two structural layers by wax printing and origami-folding, and performed colorimetric detection on MREs-CoV, MTB and HPV oligonucleotides. The origami method for the preparation of 3D paper-based sensors is simple, fast, and allows different 3D shapes to perform different operations.<sup>108</sup> 3D paper-based devices prepared by stacking require proper alignment of multiple individual layers and sufficient contact of the hydrophilic channels of each layer.<sup>109</sup> Different from the layer-by-layer stacking described above, researchers have realized the preparation of 3D paper-based devices in single-layer paper by using a variety of preparation methods. The preparation method is mainly realized by printing different hydrophobic patterns on two sides of the same paper respectively. He *et al.*<sup>103</sup>

designed and manufactured a three-dimensional (3D) structure in a paper substrate using a laser-based direct writing technique, thereby enabling multi-step analysis through the 3D structure. This method controls the depth of the hydrophobic barrier formed in the substrate by adjusting laser writing parameters such as laser power and scanning speed. After careful design and integration, three-dimensional flow paths can be generated. Jeong *et al.*<sup>110</sup> proposed 3D- $\mu$ PAD creation on a single layer of paper by controlling the penetration of different wax inks into the paper (Fig. 2E). By printing wax inks with different diffusion properties on the paper, microchannels of different sizes can be created, enabling continuous fluid delivery and multi-step biochemical reactions with a single loaded sample solution. Li *et al.*<sup>111</sup> proposed a new method for preparing 3D paper-based devices, different from origami or adhesive tape. Patterns were printed on both sides of a sheet of paper by wax printing and the penetration depth of the wax was adjusted by controlling the density and heating time of the printed wax, thus forming multi-layer patterned channels in the substrate. The technology is compatible with conventional manufacturing techniques for 3D paper-based devices and reduces the number of layers of paper required to form 3D devices, thus making quality control of the device easier. Punpattanakul *et al.*<sup>112</sup> used an inkjet printer to successfully create a three-dimensional fluid channel network with multiple fluid channel intersections on a paper layer without complex programming. The hydrophilic pattern was printed on both sides of the paper using an inkjet printer as a protective mask, and then immersed in a non-polar solution containing a hydrophobic substance to form a hydrophobic barrier on the paper. The mask pattern helped prevent adsorption of the non-polar solution onto the printed area, thereby creating hydrophobic and hydrophilic areas on the paper. Mora *et al.*<sup>113</sup> used an opaque negative photoresist selective patterning paper sheet to achieve one-step fabrication of three-dimensional paper-based microfluidic devices on a single sheet of paper without the need for folded paper, glue or tape layers. The paper-based device prepared in this way has the advantages of being small (1.6 cm  $\times$  2.2 cm), inexpensive, only requiring a low volume amount of sample (5  $\mu$ L), and having the ability to complete the mixing and dilution in 2 minutes. In summary, the 3D modeling approach allows for efficient integration of more fluid flow channels, allowing for more complex analysis of samples on a single device.<sup>9</sup> At present, the detection and research work based on 3D paper-based sensors has been carried out for disease diagnosis, food safety and environmental monitoring.

## 4. Applications of paper-based sensors

Paper-based sensors can have many of the same advantages as paper, such as being environmentally friendly, cheap, flexible, easy to manufacture and biocompatible, and so many scientists are exploring their use in fields such as

medicine, food safety, environmental monitoring, human behavior and physiological signal collection.

### 4.1 Diagnosis

Medical detection and diagnosis methods based on microfluidic sensors have been applied to the diagnosis of a large number of diseases,<sup>36,114</sup> although this research is still mostly in the development stage.<sup>115</sup> The biocompatibility of microfluidic devices based on PDMS and polydimethylsiloxane is not satisfactory,<sup>116</sup> although paper-based microfluidic sensors have good biocompatibility as well as being disposable and easy to manufacture, providing a new platform for medical application detection.<sup>2,117-119</sup> Therefore, the appearance of paper-based microfluidics provides a new possibility for the further development of microfluidics technology. The low cost and rapid detection advantages that paper-based microfluidics have are conducive to the establishment of rapid diagnosis points in underdeveloped areas or areas with scarce medical resources.<sup>2,118,120</sup> Paper-based microfluidic detection equipment is also simple to operate and portable,<sup>121</sup> which will be of great help for rapid detection at home.<sup>122</sup> In addition, paper-based sensors have been studied early in disease diagnosis and a variety of methods have been proposed to collect results, such as colorimetric detection, fluorescence detection, chemiluminescence detection and electrochemical detection.<sup>62</sup>

Colorimetric methods are commonly used to diagnose diseases in resource-limited environments because of their speed, ease of execution, and the absence of laboratory equipment.<sup>123</sup> Although they only depend on the human eye for visual observation, colorimetric methods are susceptible to individual perception and environmental influences,<sup>124,125</sup> leading to deviations in the reading of the results,<sup>7</sup> and so colorimetric methods are usually used as semi-quantitative measurement. The earliest paper-based microfluidic devices used colorimetry to read results. Whitesides *et al.*<sup>6</sup> used photolithography to construct areas and microfluidic channels on the paper substrate, and added appropriate reagents to the test areas for biological testing (Fig. 1D). The authors tested glucose and protein to prove the biological testing function of the device. Glucose determination is based on the process where iodide is oxidized to iodine by an enzyme, and the color change from transparent to brown is related to the existence of glucose. Protein determination is based on the color change of tetra bromophenol blue when it is ionized and combined with protein. When protein is present, the color of the test area changes from yellow to blue. Since this research by Whitesides *et al.*, many researchers have researched paper-based devices based on colorimetry. Tsai *et al.*<sup>126</sup> developed a paper-based tuberculosis diagnostic analysis device by means of colorimetric detection. By using the surface plasmon resonance effect and the hybridization of the single stranded DNA probe molecule with targeted double stranded tuberculosis DNA, the color changes of gold nanoparticles can be monitored (Fig. 3A). Chen *et al.*<sup>127</sup> designed a rapid colorimetric sensing system to detect ketamine, a common drug of abuse, on a microfluidic paper



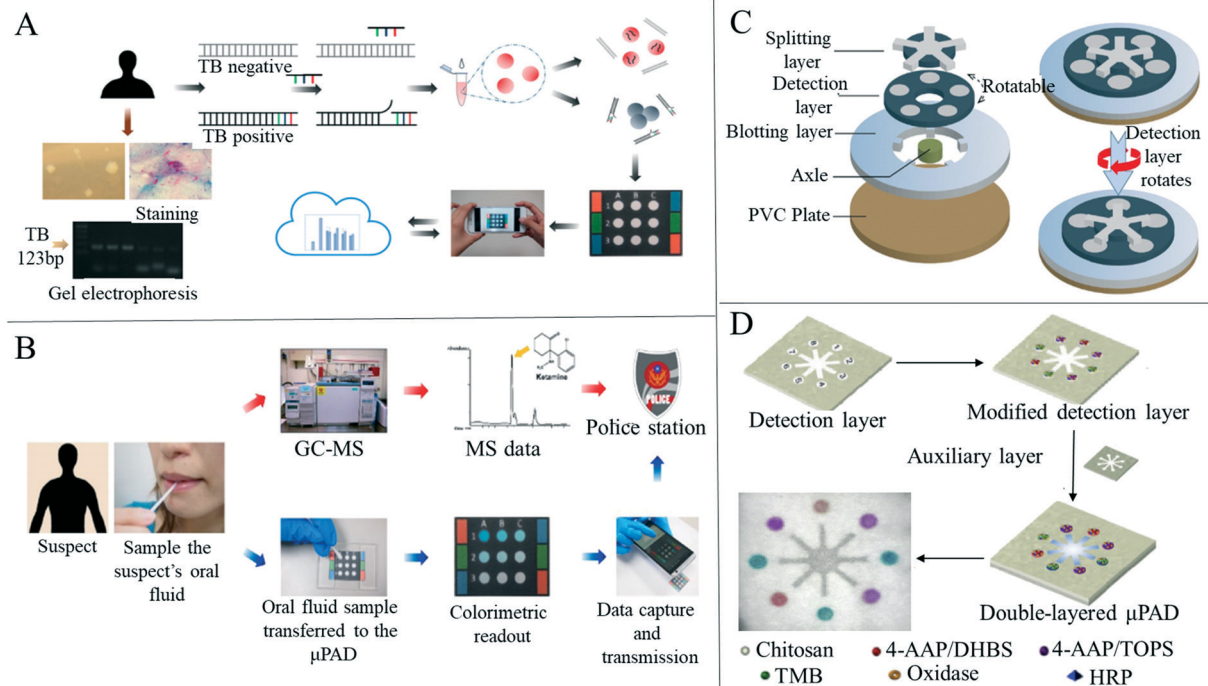


**Fig. 3** Paper-based colorimetric sensors for disease detection. (A) Schematic diagram of colorimetric diagnosis of tuberculosis and detection limit of diagnostic devices was  $1.95 \times 10^{-2}$  ng mL $^{-1}$ , and the linear dynamic range was  $1.95 \times 10^{-2}$  to  $1.95 \times 10^1$  ng mL $^{-1}$  ( $n = 5$ ). Reproduced with permission from ref. 126. Copyright 2017, American Chemical Society. (B) The schematic diagram of colorimetric detection of ketamine in paper-based analytical devices which improves the speed of ketamine analysis and reduces the cost of analysis. Reproduced with permission from ref. 127. Copyright 2019, Elsevier. (C) A multilayer diagram of a paper-based detection device for colorimetric analysis of carcinoembryonic antigens. Reproduced with permission from ref. 129. Copyright 2020, Springer Nature. (D) Schematic diagram illustrating the manufacture of two-layer paper-based devices and the simultaneous detection of four analytes and detection layers with multiple indexes. Reproduced with permission from ref. 128. Copyright 2019, Elsevier.

analysis device using competitive ELISA tests (Fig. 3B). Li *et al.*<sup>128</sup> proposed a two-layer microfluidic paper-based device with multiple colorimetric indexes for the simultaneous detection of four small biomolecules (glucose, uric acid, lactic acid and choline) within the same mixture (Fig. 3D). Wang *et al.*<sup>129</sup> developed a wax-printed multilayer paper-based microfluidic detection sensor for colorimetric detection of carcinoembryonic antigen. The device consists of a movable and rotatable detection layer to allow the microfluidic device to switch the state of the sample solution, for example, to allow the solution to flow or to be stored in the sensing area (Fig. 3C). The carcinoembryonic antigen detection limit of this device was 0.015 ng mL $^{-1}$ , and 50 positive and 40 negative human serum samples were used to successfully verify the clinical performance of this method. Nguyen *et al.*<sup>130</sup> designed a mask sensor comprising a hydration reservoir, a large surface area acquisition sample pad, a paper-based microfluidic device and a lateral flow analysis module. The sensor integrated on the mask can be used for detecting SARS-CoV-2 in human exhaled aerosol. The four modules may be located anywhere on the mask, with the requirements that the collection pad must be placed on the patient's mouth and nose inside the mask. The use of paper-based microfluidic devices enables the authors to rapidly prototype and optimize the multi-step reaction process of passive regulation. An integrated LFA strip is used to detect a

the probe cleavage in the paper-based microfluidic device assembly to realize a simple colorimetric visual readout. This SARS-CoV-2 mask sensor does not require power and operates autonomously. The sensor requires no liquid handling during the detection process and can provide visual output within 2 hours at near ambient temperature.

Paper-based devices based on fluorescence detection have also become a research hotspot in recent years. Fluorescence detection refers to qualitative or quantitative analysis of fluorescence, which can reflect the characteristics of some substances in the excited state after they are irradiated with ultraviolet light and the molecules in the excited state undergo a process of collision and emission. When some substances themselves do not emit fluorescence, or the fluorescence is very weak, it is necessary to convert non-fluorescent substances into fluorescence-emitting substances. Some reagents, such as fluorescent dyes, are used to form complexes with non-fluorescent substances.<sup>131</sup> Various complexes can emit fluorescence and therefore be measured. Fluorescence detection is highly selective, reproducible and can be qualitatively or quantitatively analyzed according to fluorescence intensity,<sup>118</sup> and so research on paper-based sensors for disease diagnosis based on fluorescence has been well explored. Liang *et al.*<sup>132</sup> developed a paper-based microfluidic device combined with a quantum dot fluorescent probe to simultaneously detect a

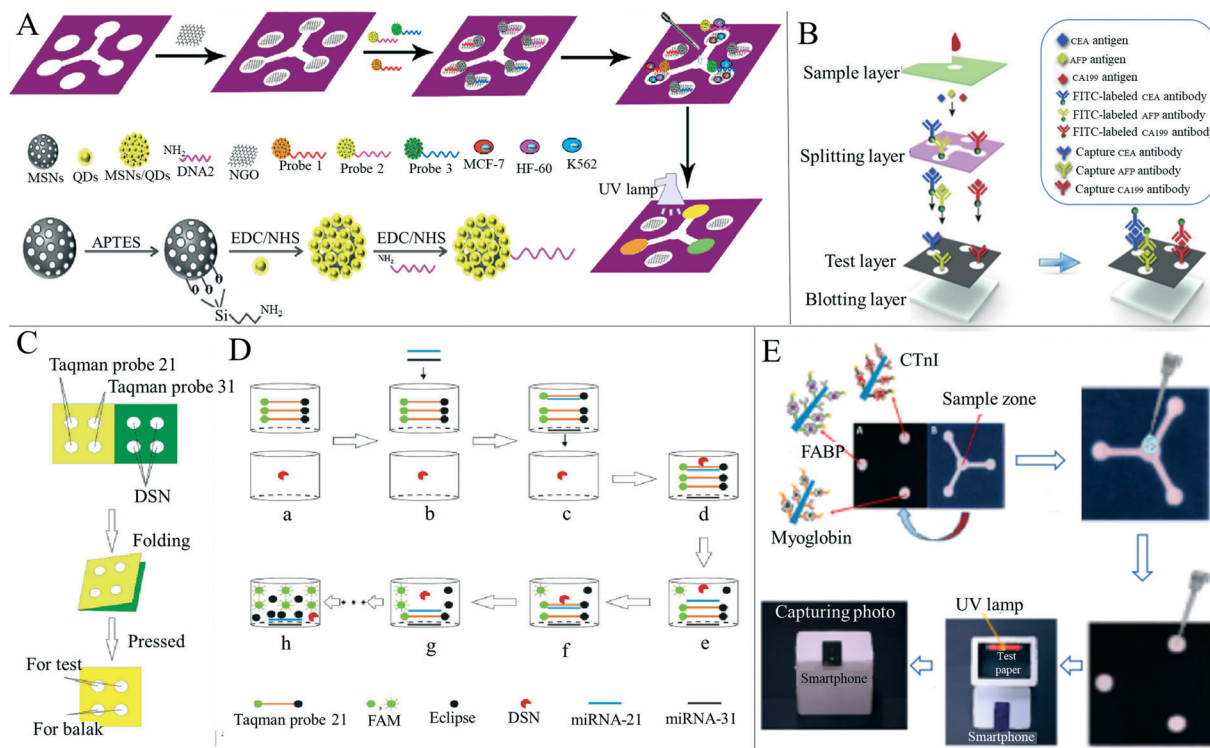


**Fig. 4** Applications of paper-based sensors for disease diagnosis based on fluorescence. (A) Schematic diagram of the whole assembly process of the paper-based cyto-sensor and probe. Reproduced with permission from ref. 132. Copyright 2016, Elsevier. (B) Simultaneous detection of three cancer biomarkers (CEA, AFP, and CA199) using a paper-based fluorogenic immunodevice. Reproduced with permission from ref. 55. Copyright 2020, Elsevier. (C) Preparation technology of a paper-based microfluidic detection device for micro-ribonucleic acid. Reproduced with permission from ref. 133. Copyright 2020, Elsevier. (D) Fluorescence amplification of MicroRNAs on paper-based microfluidic detection devices. Reproduced with permission from ref. 133. Copyright 2020, Elsevier. (E) FABP, cTnI and myoglobin were detected by a sandwich immunoassay in a portable paper-based device, and detected by an ultraviolet lamp in a homemade black box. Fluorescence image captured by a smartphone. Reproduced with permission from ref. 53. Copyright 2019, American Chemical Society.

variety of tumor cells (Fig. 4A). This method can visually observe the color change during the detection process and quantitatively analyze the number of cells. The minimum number of McF-7, HL-60 and K562 cells was 62, 70 and 65, respectively. Liang's design provides a new sensing platform for cancer cell detection that is low-cost and efficient in the real-time monitoring of multiple cancer cells. Jiao *et al.*<sup>55</sup> developed a 3D vertical flow paper-based device that uses a fluorescence immunoassay to simultaneously detect multiple cancer biomarkers (Fig. 4B). The authors introduced a vertical flow immunoassay into the device, in which the antibody labeled with fluorescein isothiocyanate was coated on the split layer and the mouse monoclonal capture antibody was functionalized on the test layer. The authors obtained good results in the detection of the three markers, where the sensitivity and accuracy met the requirements. Cai *et al.*<sup>133</sup> developed a paper-based microfluidic laser-induced fluorescence sensor based on duplex-specific nuclease amplification for the detection of MicroRNAs in cancer cells (Fig. 4C). The laser induced fluorescence detection interface was used for the first time to detect samples on paper-based chips. Under optimal conditions, the duplex-specific nuclease and TaqMan probe were retained on the circle of the folded paper. When added to the MicroRNA solution, the mixture can be cyclically digested by duplex-specific nuclease with the hybrid of

the TaqMan probe to trigger fluorescence signal amplification (Fig. 4D). Tests for mismatched miRNAs indicate that the method has good specificity. When miRNA-21 and miRNA-31 in A549 and HeLa cancer cells and LO<sub>2</sub> lysates of liver cells were measured, miRNA-21 and miRNA-31 could be successfully found from the two cancer cells and a good recovery rate was obtained, demonstrating that this device is effective, selective and sensitive for the determination of miRNAs in cancer cells and showing the feasibility of rapid and inexpensive detection of death-causing diseases such as acute myocardial infarction<sup>134</sup> and cancer,<sup>135</sup> and other diseases. So far, despite the rapid development of paper-based detection devices, there are still problems of insufficient sensitivity and accuracy.<sup>35</sup> Based on these problems, Guo *et al.*<sup>53</sup> developed a paper-based microfluidic fluorescence immunoassay device that can be used to simultaneously detect three cardiac biomarkers for acute myocardial infarction (Fig. 4E). The use of zinc oxide nanowires improved the fluorescence detection sensitivity of the final device due to the large surface area of zinc oxide nanowires, providing more binding sites, leading to an increase in the number of adsorbed fluorescent labels and a decrease in the detection limit of bio-molecules.<sup>136</sup>

In addition to colorimetric and fluorescence methods, there are also researchers who have used chemiluminescence on



paper-based sensors for medical detection. For example, Wang *et al.*<sup>137</sup> developed a paper-based device for ELISA by combining a microfluidic paper-based analysis device with chemiluminescence (Fig. 5A). The paper device was fabricated by wax printing and modified with chitosan so that the antibodies could be covalently fixed. The paper-based chemiluminescence-ELISA test was successfully carried out using tumor markers, and the linear ranges of detection of  $\alpha$ -fetoprotein, cancer antigen 125 and carcinoembryonic antigen were 0.1–35.0 ng ml<sup>-1</sup>, 0.5–80.0 U ml<sup>-1</sup> and 0.1–70.0 ng ml<sup>-1</sup>, respectively. Zhao *et al.*<sup>73</sup> introduced a paper-based immune device based on a novel protein immobilization method for

oxygen plasma treatment. The paper-based immune detection of human serum carcinoembryonic antigen was successfully performed using the clamping chemiluminescence immunoassay in the linear range of 0.1–80.0 ng ml<sup>-1</sup> and the detection limit was 0.03 ng ml<sup>-1</sup>, 30 times lower than the clinical carcinoembryonic antigen level. Zhang *et al.*<sup>138</sup> synthesized copper(II)-containing metal-organic xerogels (Cu-MOXs) with excellent catalytic performance in a luminol-H<sub>2</sub>O<sub>2</sub> chemiluminescence system, although they found that dopamine can inhibit this catalytic performance and so, based on this phenomenon (Fig. 5B), the authors established a paper-based sensitive chemiluminescence device to detect dopamine.

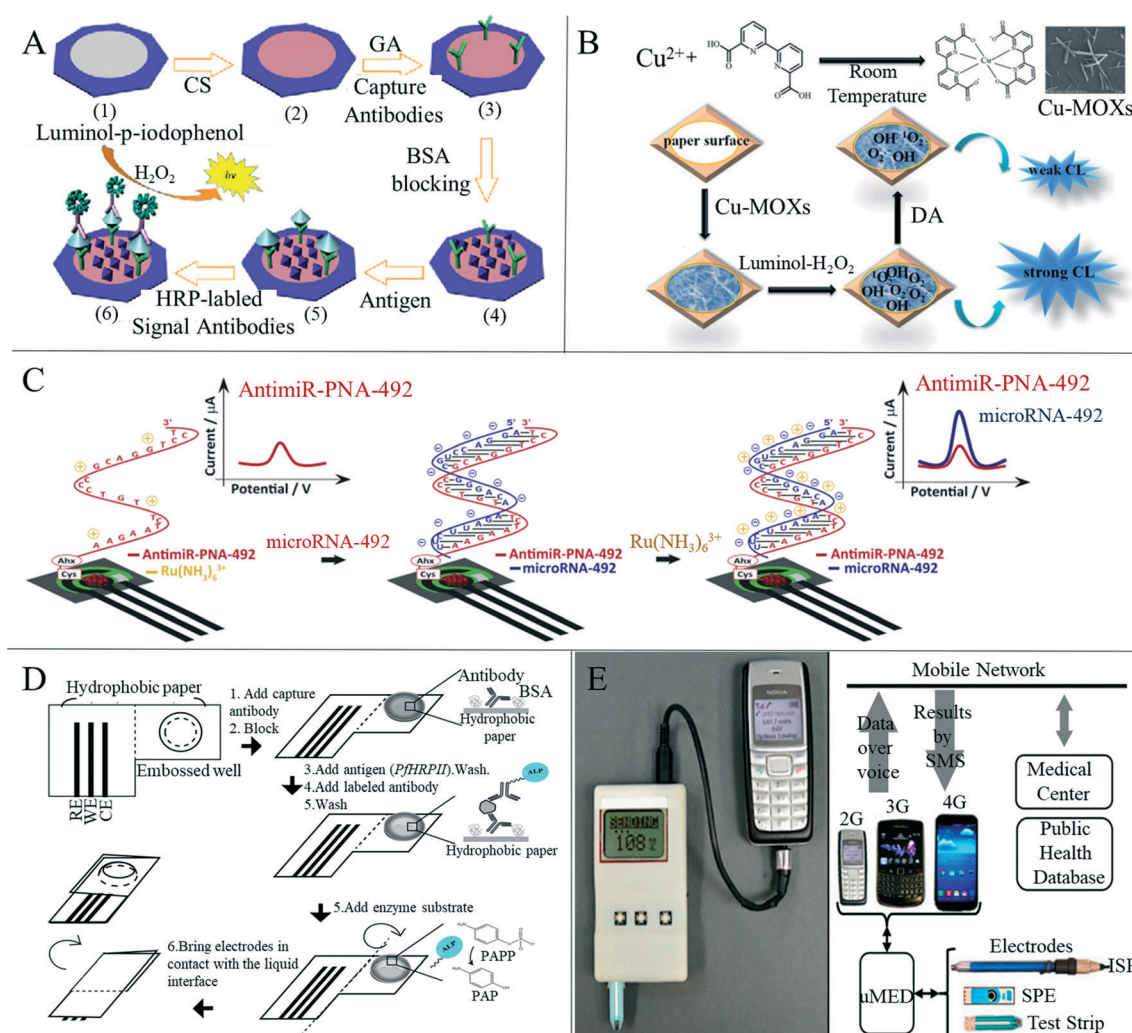


**Fig. 5** Applications of paper-based sensors for disease detection based on chemiluminescence and electrochemical methods. (A) Schematic representation of the fabrication and assay procedure for this paper-based sandwich CL-ELISA on paper immunoplate. (1) Wax-screen-printed paper zone; (2) chitosan modified paper zone; (3) capture antibodies immobilized on the paper zone through glutaraldehyde cross-linking; (4) BSA blocked paper zone; (5) paper zone after incubation with antigen solution; (6) paper zone after incubation with HRP-labeled signal antibodies and triggering CL reaction. Reproduced with permission from ref. 137. Copyright 2012, Elsevier. (B) Schematic diagram of paper-based chemiluminescence detection of DA with the luminol-H<sub>2</sub>O<sub>2</sub>-Cu-MOXs system. Reproduced with permission from ref. 138. Copyright 2020, Royal Society of Chemistry. (C) Schematic representation of the paper-based electrochemical PNA platform for the detection of miRNA-492. Reproduced with permission from ref. 143. Copyright 2020, Elsevier. (D) Schematic diagram of the microwave electrochemical immunoassay method for hydrophobic paper. Reproduced with permission from ref. 52. Copyright 2014, American Chemical Society. (E) Schematic diagram of the universal mobile electrochemical detector and the connection from the electrode to the network. Reproduced with permission from ref. 148. Copyright 2014, National Academy of Sciences.



They obtained a linear range of 40–200 nM and a detection limit of 10 nM for dopamine, and confirmed that this method can be used to determine dopamine in urine samples.

Electrochemical detection has become a commonly used detection method in paper-based disease detection due to its low cost, high sensitivity and high selectivity, especially for the detection of various blood analytes.<sup>139</sup> Paper-based devices based on electrochemical analysis were first proposed by Dungchai *et al.*<sup>140</sup> in 2009. With the continuous development and improvement of paper electrochemical detection equipment, applications in medical diagnosis have been under development. Glavan *et al.*<sup>52</sup> described a device for electrochemical enzyme-linked immunosorbent assay (Fig. 5D) that was completely made of hydrophobic paper, made by silanization of paper with decyl trichlorosilane, and included two areas separated by a central crease. The surface of the paper was fixed and recognized by antigens or antibodies. The device was folded along the central crease to bring the two areas into contact and the analytical signal from the folded configuration was recorded. The authors used electrochemical direct ELISA for detecting rabbit antigen IgG in the buffer and electrochemical sandwich ELISA for detecting malaria histidine-rich protein in *Plasmodium falciparum* in spiked human serum, demonstrating the versatility of this device. Cinti *et al.*<sup>141</sup> developed a paper-based biosensor containing Prussian blue nanoparticles and glucose oxidase for electrochemical detection of glucose in the blood. The biosensor had a wide range of dynamic responses up to 25 mM (450 mg dL<sup>-1</sup>) and a correlation coefficient with commercial glucose test paper of 0.987, indicating that the device is capable of effectively detecting blood glucose. This device provides a new and convenient method for self-monitoring of diabetes patients. Boonkaew *et al.*<sup>142</sup> have created a label-free electrochemical immune sensor for the detection of ferritin using a paper-based analysis device. In the presence of ferritin, the sensor showed a considerable decrease in electrochemical response in a concentration-dependent manner. Satisfactory results have been obtained in the detection of ferritin in human serum, indicating that this paper-based immune sensor may be a substitute device for the diagnosis of iron deficiency anemia. Moccia *et al.*<sup>143</sup> reported a cost-effective paper-based electrochemical peptide nucleic acid biosensor for the detection of miRNA-492, a biomarker for pancreatic duct adenocarcinoma (Fig. 5C). Using a novel highly specific peptide nucleic acid as the recognition element, the authors evaluated the formation of the PNA/miRNA-492 admixture by monitoring the interaction between positively charged ruthenium(II) hexamine and uncharged and/or negatively charged PNA/miRNA-492 duplex. Excellent selectivity to single and double base mismatch (1MM, 2MM) or scrambled sequences was highlighted, and miRNA-492 was measured in undiluted serum, demonstrating its applicability in biomedical analysis. e Silva *et al.*<sup>144</sup> developed an electrochemical paper-based analytical device for the simple, inexpensive and sensitive detection of *Pseudomonas aeruginosa* for early infection. Maier *et al.*<sup>145</sup> prepared a disposable paper-based electrochemical wearable sensor that can be integrated

into a commercial respiratory mask to detect hydrogen peroxide in human expired air. The accuracy of hydrogen peroxide detection was improved by differential electrochemical measurement using screen-printed Prussian blue-mediated and non-mediated carbon electrodes. Different from previous work, this detection form combined with the mask realizes wearable detection, which is beneficial for real-time and continuous detection of human exhaled air.

Although many researchers continue to study paper-based sensors with wider detection ranges and higher sensitivity, there is also a trend of developing paper-based sensors that can interface with portable devices to remove the need for large medical devices and professional medical personnel.<sup>146</sup> Nie *et al.*<sup>147</sup> combined a simple electrochemical micro-paper analysis device with a commercial blood glucose meter to conduct a rapid and quantitative electrochemical analysis of many compounds related to human health, such as glucose, cholesterol, lactic acid and alcohol, in blood or urine. Nemirovski *et al.*<sup>148</sup> designed a universal mobile electrochemical detector based on paper, which can be used for medical testing in resource-constrained areas (Fig. 5E). The device is compatible with a variety of electrode formats, the mixing of samples in a vibrating manner and the detection of data *via* voice transmission. This method ensures connection with any mobile phone, from low-end phones to smart-phones, or cellular networks. This method can be used to carry out rapid medical tests in remote and underdeveloped areas, and the test results can be sent to doctors in real time through a mobile phone network, which is expected to help the establishment of rapid medical test points in remote areas. These technological advances offer great promise for the transformation of paper-based electrochemical analysis devices from laboratory proof-of-concept equipment to saleable and commercially manufactured equipment.<sup>149</sup>

#### 4.2 Paper-based wearable sensors for human physiological and behavioral signal monitoring

Flexible wearable devices have great potential in the fields of human behavior perception, physiological information monitoring and human-computer interaction, and flexible sensors have attracted increased interest due to their importance in wearable devices. Since the COVID-19 worldwide epidemic in 2019, the potential of wearable health devices with flexible sensors has become more obvious.<sup>150</sup> Traditional flexible sensors mainly consist of polymer materials as flexible bases, such as polydimethylsiloxane and polyethylene terephthalate. These polymer materials have high durability, but often come with problems, such as high cost, poor permeability and poor degradability. In recent years, researchers have used paper-based sensors as electronic skin to detect information related to the human body, such as pulse, respiration, pronunciation and body behavior; they can also help the human body to perceive changes in pressure, temperature and humidity from the surrounding environment.



The detection of these kinds of information will benefit personalized medicine, real-time analysis of physical conditions, posture correction and many other medical applications, and could also be used to connect with machines to realize human-computer interactions.

Recently, human behavior and physiological paper-based sensing has been thoroughly researched. Gao *et al.*<sup>11</sup> prepared

an all paper-based piezoresistive pressure sensor, using paper coated with silver nanowires as the sensing layer and nanocellulose paper as both the bottom substrate and top packaging layer of the printed electrode (Fig. 6A). The sensor provided good signal feedback in both bending and pressing scenarios, and was installed on human skin to monitor physiological signals, such as arterial heart pulses and throat

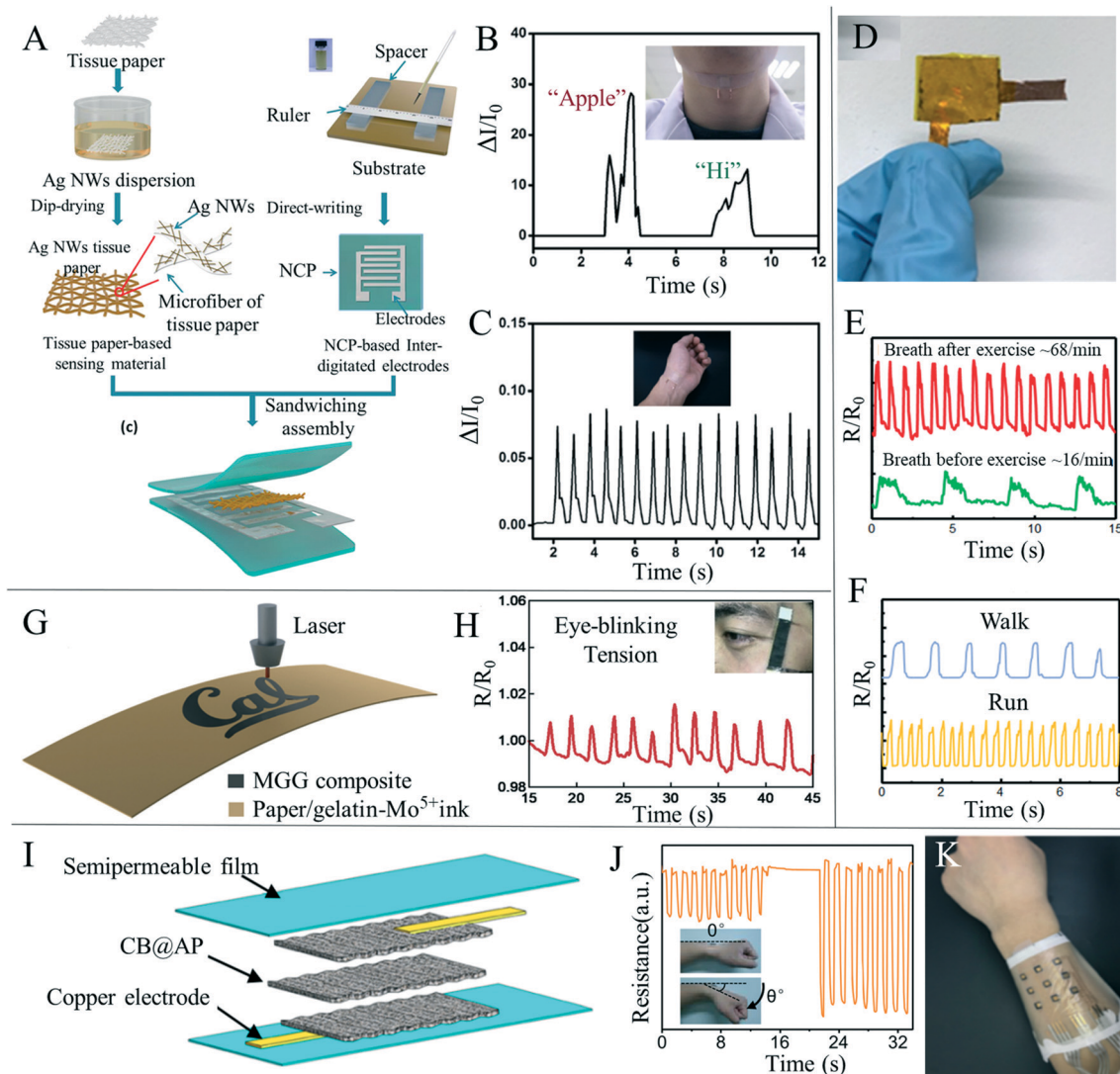


**Fig. 6** Paper-based mechanical sensors for human body monitoring. (A) Schematic drawing of all paper-based flexible and wearable piezoresistive pressure sensors. Reproduced with permission from ref. 11. Copyright 2019, American Chemical Society. (B) The arterial heart pulse was measured on the wrist, and the pulse was 75 times per minute. Reproduced with permission from ref. 11. Copyright 2019, American Chemical Society. (C) Response curve of the pressure sensor installed in the throat to monitor pronunciation. Reproduced with permission from ref. 11. Copyright 2019, American Chemical Society. (D) Photos of the graphene/paper-based pressure sensor packaged with PI. Reproduced with permission from ref. 151. Copyright 2017, American Chemical Society. (E) Responsive curves of breathing before and after exercise. Reproduced with permission from ref. 151. Copyright 2017, American Chemical Society. (F) Response curves of walking and running in sports monitoring. Reproduced with permission from ref. 151. Copyright 2017, American Chemical Society. (G) Direct laser writing process of the molybdenum-graphite composite material on the paper substrate (gelatin-Mo<sup>5+</sup> ink was absorbed on the top surface of the paper and turned into the molybdenum-graphite composite via the laser printing process). Reproduced with permission from ref. 155. Copyright 2020, Elsevier. (H) Paper-based sensor based on molybdenum carbide-graphene detects the change of resistance during blinking. Reproduced with permission from ref. 155. Copyright 2020, Elsevier. (I) Schematic diagram of the flexible multi-layer carbon black and airlaid paper pressure sensor. Reproduced with permission from ref. 156. Copyright 2019, American Chemical Society. (J) The signal response of the sensor fixed on the back of the wrist under different degrees of cyclic bending. Reproduced with permission from ref. 156. Copyright 2019, American Chemical Society. (K) Wearable arrayed electronic skin can be connected to human arms. Reproduced with permission from ref. 156. Copyright 2019, American Chemical Society.



sounds, (Fig. 6B and C) and can act as a flexible electronic skin in response to external pressure. Tao *et al.*<sup>151</sup> prepared a paper-based, high-performance pressure sensor by converting a multilayer mixed graphene solution and paper material into multilayer graphene paper by means of thermal reduction (Fig. 6D). The sensor made use of the air passage between graphene paper layers and the unique microporous structure of the paper material, as the resistance of graphene paper significantly changed under the action of pressure, thus greatly improving the pressure sensitivity by selecting the appropriate type of graphene paper and the number of layers of the paper, and the sensitivity could be further improved and accurate detection of pulse, respiration and various motion states could be achieved (Fig. 6E and F). Zhang *et al.*<sup>152</sup> used facial tissues to create a new wearable sensor that can detect pulse, blinking and other types of human movement. The sensors were lightweight, flexible and cheap, and could be used in areas such as healthcare, entertainment and robotics. Based on the porous microstructure of the paper, the conductive current of the device was regulated by the change of the contact area between layers under pressure, enabling the capture of and feedback from the external stress stimulus. Yang *et al.*<sup>153</sup> simply achieved the preparation of new mechanical sensors with excellent stability by impregnating paper with poly (3,4-ethyldithiophene)-polystyrene sulfonate (PEDOT:PSS) solution. Wang *et al.*<sup>154</sup> developed a super-sensitive pressure sensor with a wide measurement range using a carbon nanotube homogeneous solution sprayed directly on the paper surface as the sensing material. Due to the large specific surface area of the carbon nanotube, the porous structure of the paper, and the synergistic effect of effective contact between the carbon nanotube and the intercalated electrode, the pressure sensor achieves a wide measurement range from 0 to 140 kPa and exhibits good stability over 15 000 test cycles. Similarly, Long *et al.*<sup>155</sup> prepared a porous and stacked molybdenum-graphene carbide composite on a paper-based substrate as a piezoelectric resistive strain/pressure sensor (Fig. 6G). The device could detect not only the amplitude and frequency of the applied strain, but also the direction of stretched or compressed deformation. The sensor was applied to detect the opening and closing of the eyes, the flexion of elbow muscles (Fig. 6H), and the laryngeal movement of different words under conditions such as drinking laryngeal movement and silence, and obtained good signal output. Han *et al.*<sup>156</sup> prepared an ultra-low cost, high sensitivity and flexible pressure sensor by drop coating carbon black on dust-free paper (Fig. 6I) that was used to detect pulse, voice and wrist bending cycle (Fig. 6J). The flexible electronic skin can be attached to the surface of the human body to respond to external stimuli (Fig. 6K). Paper-based mechanical sensors have also been used in daily monitoring of the human body. Strong results have been achieved in measuring various limb behaviors, pulse and sound detection, although there are still issues including the need for an external wired power supply and signal reception, greatly limiting its convenience in daily

detection, and so the development of battery or wireless power supply and wireless signal transmission are key research focuses.

Sweat is often used as a test sample, reflecting some physiological information of the tested person by detecting the content and change of certain substances in the sweat.<sup>157</sup> In addition, sweat can be easily obtained through sweat glands all over the body, making it a suitable medium for integrated non-invasive detection.<sup>158</sup> Paper-based sensors are often used to fabricate sweat detection sensors due to their porous, easy-to-fabricate fluid channels and capillary action. Parrilla *et al.*<sup>159</sup> detailed a wearable paper-based sensor for monitoring sweat dynamics including sweat rate and sweat loss. The sensor integrates a single-walled carbon nanotube and a surfactant (sodium dodecyl benzene sulfonate) nanocomposite into a cellulose fiber of conventional filter paper as a sensing layer. The authors first demonstrated sweat release monitoring during cycling under laboratory conditions, followed by usage with a wireless multimeter and mobile handset to demonstrate true wearable applications (Fig. 7A and B). Wu *et al.*<sup>160</sup> proposed a new paper-based sweat generator with an alternating electrode structure (Fig. 7C), which utilized the interaction between electrodes and sweat in the redox reaction to generate electricity. In addition, the output current of the device correlated with lactate content in human sweat (Fig. 7D), suggesting its potential application as a human healthcare device. Xu *et al.*<sup>161</sup> have developed a method to make flexible electronic devices using pencil and paper (Fig. 7E). Their devices include temperature sensors, electrophysiological sensors, electrochemical sweat sensors, Joule heating elements and humidity generators. Among them, the electrochemical sweat sensor monitored pH, uric acid and glucose in sweat with high sensitivity and selectivity (Fig. 7F and G). Ortega *et al.*<sup>162</sup> integrated a disposable bio-sensor with a glucose/oxygen enzyme fuel cell made on a small piece of paper, where the entire detection system could be attached to an ordinary sized band-aid (Fig. 7H). The paper battery component used by the authors in the device was activated upon absorbing sweat (Fig. 7I). When the paper-based detector was attached directly to the skin, sweat from the skin was drawn into the device, converting the chemical energy produced by glucose oxidation into electrical energy and allowing glucose levels to be monitored without the need for external power sources and complex readout devices. Finally, that authors' experiment showed that a sample representing a "healthy" patient produced voltages in all devices under test that were below the threshold of the transistor and the display was not lit. Conversely, the display was activated in "non-healthy" patients due to voltages over the threshold being yielded. (Fig. 7J). The authors also compared the test results with the known diagnosis and showed that the device can produce 95% sensitivity and 100% specificity (Fig. 7K).

In recent years, the efficient detection of sensor elements has become a research hotspot, and researchers have gradually carried out the research work that a single paper-



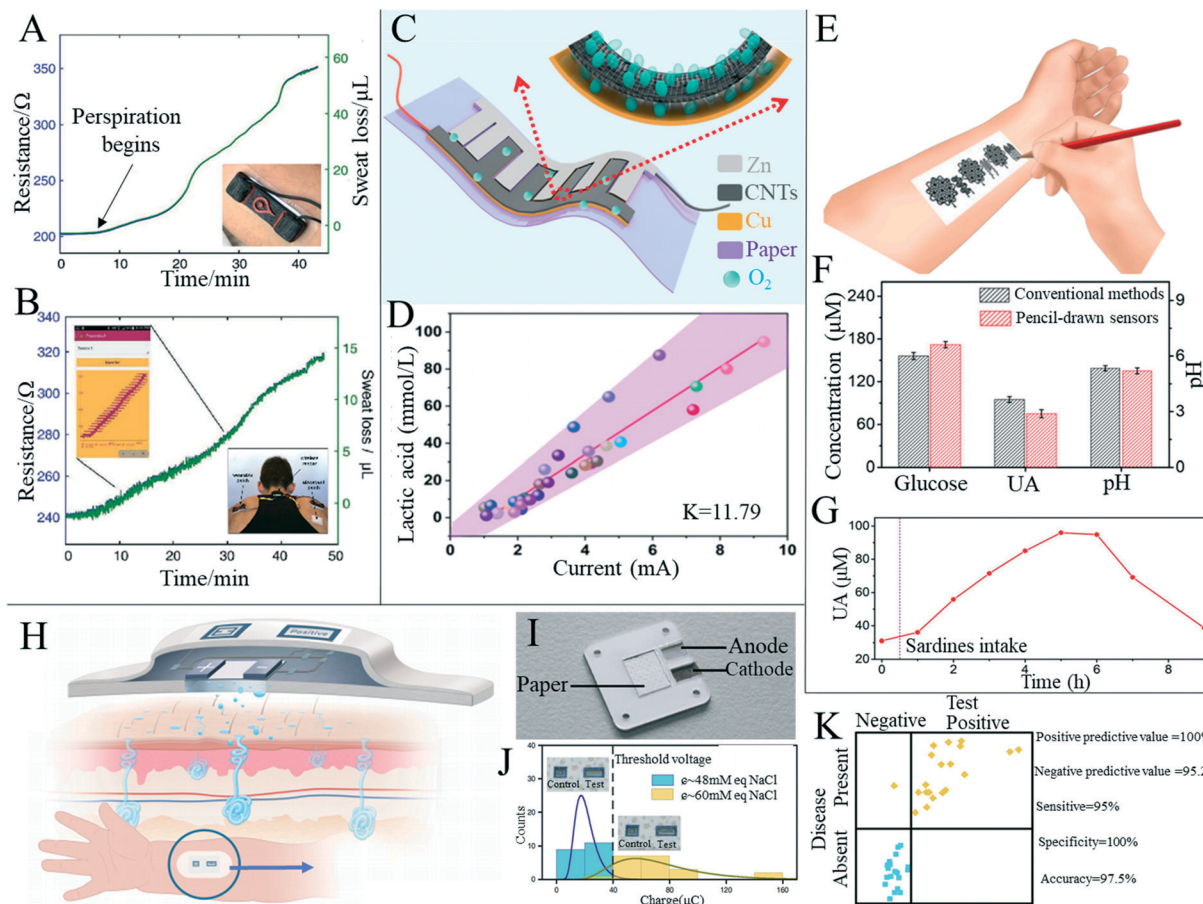


**Fig. 7** Paper-based sensors for daily monitoring of human sweat. (A) Sensor for monitoring perspiration dynamics in real time (insert illustration shows the patch attached to the participant's skin). Reproduced with permission from ref. 159. Copyright 2019, Wiley-VCH. (B) Paper-based sweat sensor used to monitor the rider's sweat condition in real time through a wireless reader and mobile phone interface. Left insert shows screenshots of the mobile phone application obtained in the physical test and right insert shows back photos of the subjects while riding. All sweat loss charts were recorded in cycling practice. Reproduced with permission from ref. 159. Copyright 2019, Wiley-VCH. (C) Schematic diagram of a wearable sweat-based generator. Reproduced with permission from ref. 160. Copyright 2020, American Chemical Society. (D) Relationship between lactic acid content in sweat and output current of the paper-based sweat generator. Reproduced with permission from ref. 160. Copyright 2020, American Chemical Society. (E) Conceptual diagram of an electronic device on paper using a sketching pencil. Reproduced with permission from ref. 161. Copyright 2020, National Academy of Sciences. (F) Comparison of data of three substances in sweat measured by the paper-based sensor with the traditional method. Reproduced with permission from ref. 161. Copyright 2020, National Academy of Sciences. (G) Paper-based UA sensor records the dynamic changes of UA concentration before and after purine-rich food was eaten by test subjects. Reproduced with permission from ref. 161. Copyright 2020, National Academy of Sciences. (H) Automatic force skin patch design and theoretical working scenario for measurement of sweat-wicking conductivity. Reproduced with permission from ref. 162. Copyright 2019, Springer Nature. (I) Paper-based battery components in the patch. Reproduced with permission from ref. 162. Copyright 2019, Springer Nature. (J) Gaussian distribution of accumulated charge at conductivity of healthy and unhealthy samples. Reproduced with permission from ref. 162. Copyright 2019, Springer Nature. (K) Comparison of results provided by all paper-based devices with known conditions (healthy and unhealthy) of samples. Reproduced with permission from ref. 162. Copyright 2019, Springer Nature.

based sensor can detect a variety of signals. Luo *et al.*<sup>163</sup> combined paper-based sensing technology with a direct laser writing method to design and manufacture a simple and wearable sensor based on the polyimide/paper double-layer structure (Fig. 8A and B). The polyimide/paper double-layer thin-film sensor has been successfully used to monitor pulse and respiratory activity and was used as a dual sensor to detect both force and humidity stimuli (Fig. 8C and D). Liu *et al.*<sup>164</sup> developed a paper-based sensor that could simultaneously measure four physical conditions. A water-based dispersion of carbon black/reduced graphene was

sprayed onto the paper, which dried to form a sensing layer on the paper, and finally copper wires were introduced at both ends to form a multifunctional paper-based sensor (Fig. 8E). The paper-based sensor was used to detect changes in strain, temperature, humidity and pressure, proving the multi-functional applicability of the sensor (Fig. 8F). The sensor was easy to prepare, had easy degradation in water and reusability, and could be widely used in health monitoring, human machine interfaces, soft robotics, wearable devices and intelligent control technologies. Jo *et al.*<sup>165</sup> successfully developed a glycerin paper-based sodium

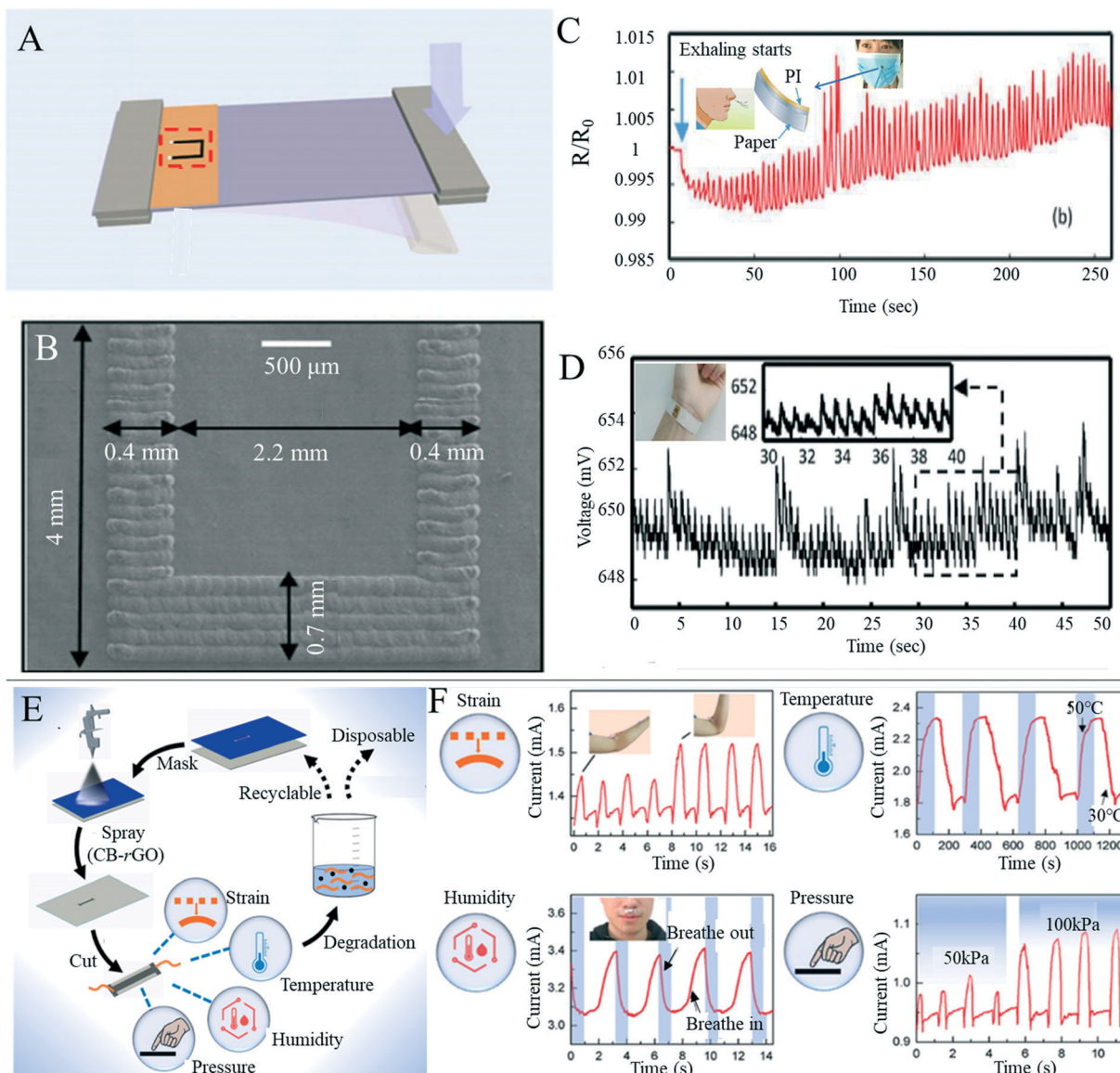


**Fig. 8** Multifunctional applications of paper-based sensors. (A) Cantilever force sensor design based on the PI/paper bilayer membrane (prominent U-shape is graphite structure produced by carbon dioxide laser irradiation). Reproduced with permission from ref. 163. Copyright 2018, Royal Society of Chemistry. (B) Scanning image of the u-shaped graphite structure of the double-layer film irradiated by a carbon dioxide laser. Reproduced with permission from ref. 163. Copyright 2018, Royal Society of Chemistry. (C) Humidity sensor based on the PI/paper bilayer film records the resistance changes during exhalation and inhalation. Embedded display is a prototype respiratory sensor assembled from a mask and sensor. Reproduced with permission from ref. 163. Copyright 2018, Royal Society of Chemistry. (D) The pulse sensor wrapped around the wrist is used to monitor the resistance change during pulse, excited by 1 mA current. Embedded display is a prototype of the pulse sensor made by sticking a polyimide/paper double-layer film on the back of adhesive tape. Reproduced with permission from ref. 163. Copyright 2018, Royal Society of Chemistry. (E) Schematic diagram of the preparation process of the multi-modal paper-based sensor. Reproduced with permission from ref. 164. Copyright 2019, American Chemical Society. (F) Multi-modal paper-based sensors are used to detect changes in strain, temperature, humidity and pressure. Reproduced with permission from ref. 164. Copyright 2019, American Chemical Society.

silicate nanogenerator with antimicrobial properties and water solubility using a simple vacuum filtration method. The sensor could be attached to the skin as an electronic skin to detect human movement or sense external stimuli, as well as having antibacterial effects. Although paper-based sensors with multiple functions are constantly being developed, there are still some problems with rapid development. There is still a certain gap between the

durability and sensitivity of sensors prepared with traditional substrates. Multi-function detection often uses a single device to realize the separate detection of multiple detection data, but cannot analyze and process multiple pieces of detection information simultaneously. In addition, the tensile property of paper is poor, which limits the preparation of tensile strain sensors based on paper. Therefore, the preparation of more integrated paper-based sensors, the development of

new paper types and the improvement of durability would be worthwhile research directions of paper-based sensors in the future.

#### 4.3 Food safety detection

Food safety incidents occur globally, and toxic or harmful food can seriously impact health and wellbeing, making food safety of interest to everyone.<sup>166</sup> Testing at every step of the food manufacturing process is vital to ensure that safe, acceptable and beneficial food reaches every consumer.<sup>167</sup> In the research and preparation of sensors for food safety analysis, paper-based sensors are of great interest; because of its low price and ability to fix or freeze-dry various biomolecules to its hydrophilic surface without great effort, paper is a good substitute for other substrate materials.<sup>1</sup> However, there are not many mature paper-based sensors for

food quality analysis in the market at present, with the majority still being in the laboratory stage.

With the improvement of living standards and availability of produce, more attention is paid to diet and the nutritional content of food. Beverages, such as milk, fruit juices and vegetable juices, have become essential products in our daily life, but issues including adulteration, excessive additives, insufficient processing and bacterial contamination can occur frequently. Mahato *et al.*<sup>168</sup> developed a paper-based immune sensor for the detection of alkaline phosphatase in milk products (Fig. 9A). The device could be semi-quantitatively analyzed by the naked eye, and quantitative estimation was made by combining digital image colorimetry with smart phone technology, where the dynamic range of alkaline phosphatase detection was 10–1000 U mL<sup>-1</sup> and the detection limit was 0.87 ( $\pm 0.07$ ) U mL<sup>-1</sup>. Zong *et al.*<sup>169</sup> have developed a low-cost and simple method for the highly sensitive and selective detection of norfloxacin in milk at the

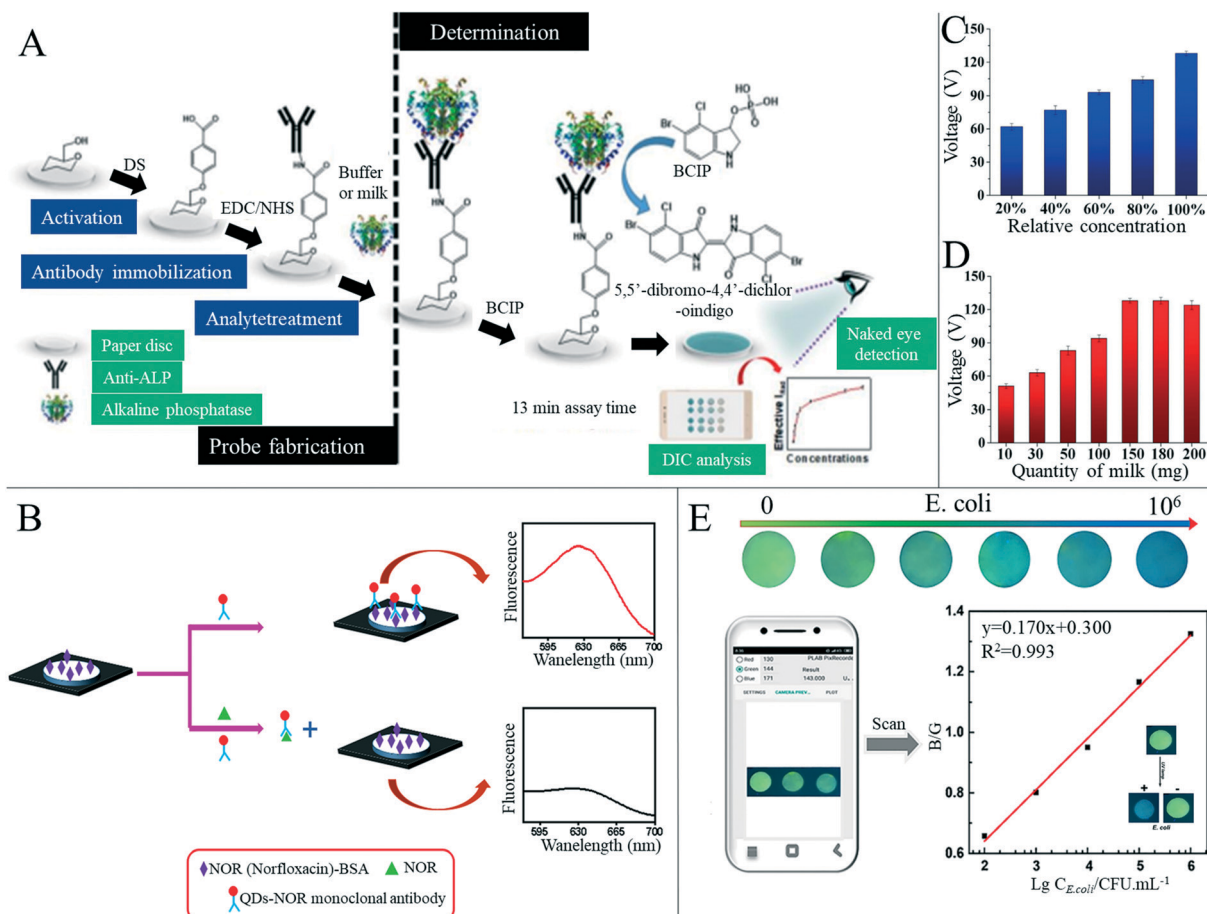


**Fig. 9** Paper-based sensors for beverage food detection. (A) Schematic diagram of production and detection principle of the alkaline phosphatase paper-based biosensor. Reproduced with permission from ref. 168. Copyright 2018, Elsevier. (B) Schematic diagram of the paper-based fluorescence immunoassay for detection of norfloxacin. Reproduced with permission from ref. 169. Copyright 2019, Elsevier. (C) Relationship between output performance of the paper-based friction generator and milk quantity. Reproduced with permission from ref. 171. Copyright 2019, Elsevier. (D) Relationship between output performance of the paper-based friction generator and relative concentration of milk. Reproduced with permission from ref. 171. Copyright 2019, Elsevier. (E) Color images of paper-based sensors with different concentrations of *E. coli* under 302 nm ultraviolet light were analyzed using a smartphone APP to detect *E. coli*. The illustration in the figure shows the recognition of *Escherichia coli* by the paper-based vision sensor based on the OPD-Cu<sup>2+</sup> system. Reproduced with permission from ref. 124. Copyright 2020, Springer Nature.

picogram level through a paper-based fluorescence immunoassay (Fig. 9B). Norfloxacin was detected quantitatively in paper-based devices by using quantum dot labeled monoclonal antibodies as detection probes to identify the corresponding norfloxacin. The detection limits of aqueous solution and milk were  $1 \text{ pg mL}^{-1}$  and  $10 \text{ pg mL}^{-1}$ , respectively. The paper-based fluorescence detection device provided a cheap, sensitive, environmentally friendly and rapid method for the quantitative detection of norfloxacin in milk and has a broad application prospect in food safety detection. Some researchers have also started research on the detection of nutritional value in beverages. Silva *et al.*<sup>170</sup> reported a new paper-based sensing platform and its application in an unlabeled potential-immune sensor for *Salmonella typhimurium* detection based on the blocking surface principle. The potential shift resulting from the ion flux blocking effect caused by antigen–antibody binding was correlated with the logarithm of *Salmonella typhimurium* concentration in the sample. Under optimal conditions, the detection limit of 5 cells per ml was reached. The authors also applied the sensor to detection in apple juice samples, concluding the sensor's potential for practical applications. Xia *et al.*<sup>171</sup> developed a new, efficient, milk-paper-based friction nanogenerator with a simple structure, small size, low cost and high speed. In addition to collecting mechanical energy generated by human movement, the nanogenerator could also be used to detect the concentration of milk according to the relationship between milk volume and output performance. The authors firstly set the original concentration of milk to 100%, and prepared milk with a relative concentration of 20%, 40%, 60% and 80% in water, where the final output voltage increased with the increase of milk concentration (Fig. 9C and D). Sha *et al.*<sup>172</sup> assembled Au @AG core–shell nanoparticles on filter paper as a substrate for surface-enhanced Raman spectroscopy for rapid field detection of estazolam in beverages. The lowest EST detection concentration in aqueous solution was as low as  $5 \text{ mg L}^{-1}$ , and EST components in orange juice and pomegranate juice could be effectively detected by simple pretreatment where the lowest EST detection concentration was  $10 \text{ mg L}^{-1}$ , with good signal uniformity. Wang *et al.*<sup>124</sup> developed a paper-based device capable of simultaneous fluorescence and colorimetric detection for detecting food-borne pathogens. Food-borne pathogens such as *Escherichia coli* can cause serious diseases such as hemorrhagic diarrhea, hemolytic uremic disease and even death by contaminating food such as vegetable juice, fruit juice and water.<sup>173</sup> The authors used  $\text{Cu}^{2+}$  to trigger the oxidation of *o*-phenylenediamine (OPD), which could oxidize OPD to OPDox to produce orange-yellow fluorescence and visible light yellow. However, *E. coli* can effectively reduce  $\text{Cu}^{2+}$  to  $\text{Cu}^+$  and inhibit the oxidation of OPD triggered by  $\text{Cu}^{2+}$  to OPDox, enabling the detection of *E. coli*. With the help of a smart phone color scanning application and the prepared sensor, the quantitative detection of *E. coli* was possible (Fig. 9E).

The use of some reagents, such as pesticides, growth promoters, clenbuterol and desiccants, can leave residues in food and could have adverse effects on consumers' health, and so the detection of adulterants and related substances in food is of great importance.<sup>174</sup> Ma *et al.*<sup>175</sup> developed a paper-based microfluid enzyme linked immunosorbent assay for the rapid detection of clenbuterol hydrochloride, illegally used as a growth stimulant in food-producing animals. Clenbuterol was detected by measuring the intensity of the color change, which was proportional to the concentration of the analyte, and the detection limit was 0.2 ppb. The device effectively reduced the cost, dosage and time required to run ELISA for food sample testing. Wang *et al.*<sup>176</sup> developed a sensitive monoclonal antibody (mAb) against toltrazuril based on a novel hapten. A colorimetric paper-based sensor was produced for rapid screening of toltrazuril and its metabolites in chicken and egg samples (Fig. 10A and B). The sensitivity and accuracy of the test were up to the official standards, therefore providing a new way for a toltrazuril rapid field test. Chen *et al.*<sup>177</sup> developed a paper-based sensor based on CdTe quantum dots and nano-ZnTPyP for fluorescence detection of carbamate pesticides in food. When samples containing carbamate pesticides were added, the fluorescence of CdTeQDs quenched by nano-ZnTPyP could be effectively restored, and an “on off” detection model of carbamate pesticides was constructed. The authors also combined partial least squares discriminant analysis and partial least squares regression models to realize the quantitative and qualitative analysis of carbamate pesticides with high sensitivity and specificity in complex biological and food matrices with high sensitivity. In the authors' specificity test, the presence of metolcarb resulted in a change in the fluorescent color from dark green to yellowish green, while other pesticides remained dark green (Fig. 10C). This differential chromogenic result ensured rapid, highly sensitive, highly specific, and field detection of carbamate pesticides, and the concentrations of carbamate pesticides in apple, cabbage and tea were accurately quantified. Trofimchuk *et al.*<sup>178</sup> developed a paper-based microfluidic device for detecting nitrite in meat. The concentration of nitrite was determined by the colorimetric reaction between nitrite and Griess reagent, and the detection limit was increased by the coffee-ring effect. The detection limit of nitrite in pork by this device was  $19.2 \text{ mg kg}^{-1}$ , but could be as low as  $1.1 \text{ mg kg}^{-1}$  if the coffee ring area is analyzed. The could be completed in 15 minutes, and therefore the device has potential application in routine screening of nitrite concentration in meat products, helping to ensure food safety and consumer health. Bougadi *et al.*<sup>179</sup> developed a paper-based microfluidic device for detecting adulterated food (Fig. 10D and E). This device could detect the lowest doping rate of 0.01%, 10 times the sensitivity of other detection methods, with good reproducibility and specificity, and could be used for meat, beans and other foods for adulteration detection. Similarly, Batule *et al.*<sup>180</sup> constructed a paper-based device for rapid extraction of mitochondrial genomic



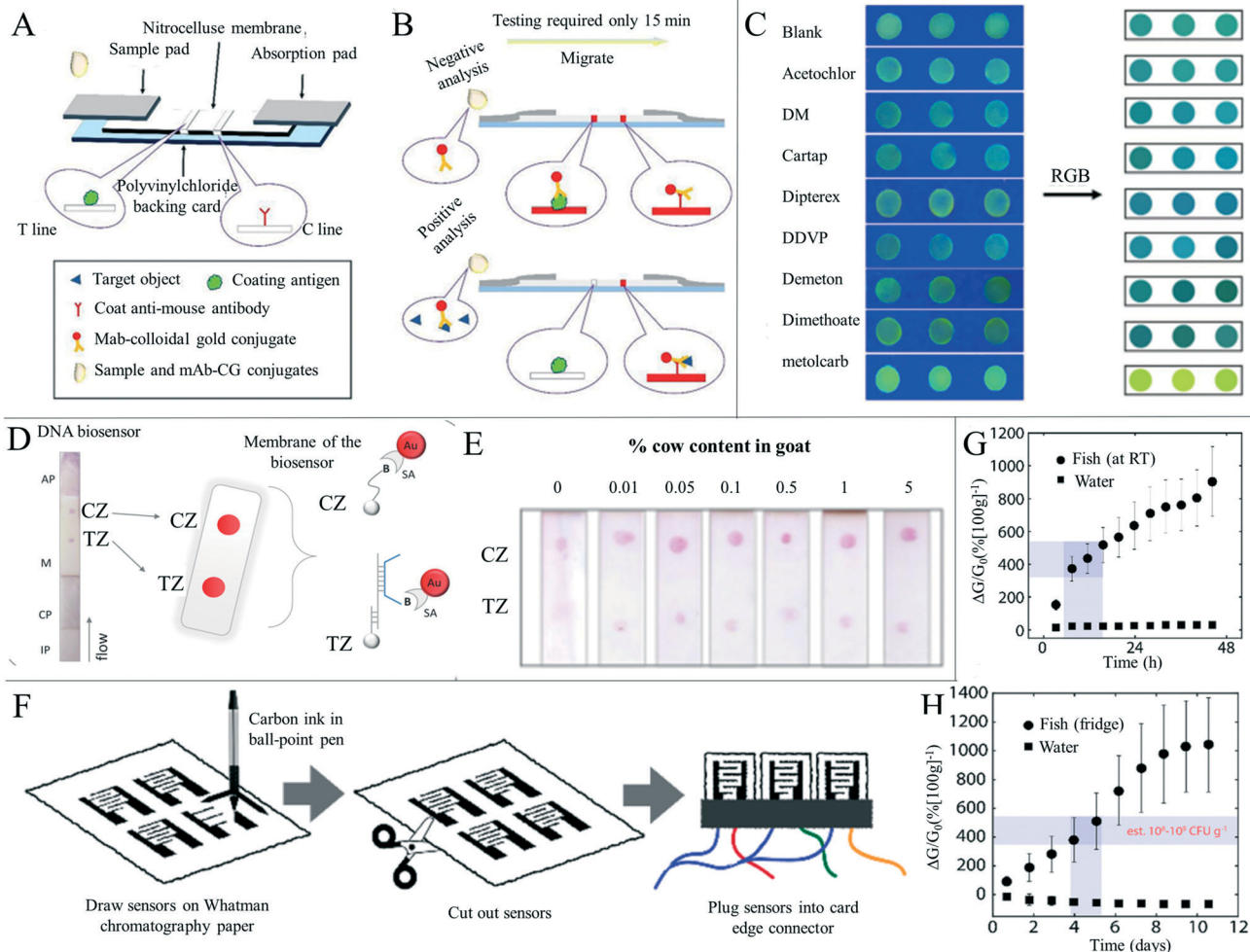


**Fig. 10** Detection of substances and freshness in foods other than beverages. (A) The structure of the paper-based colorimetric sensor for the detection of toltrazuril and its metabolites in feed, chicken and egg samples. Reproduced with permission from ref. 176. Copyright 2018, Elsevier. (B) Schematic diagram of the negative and positive samples of toltrazuril and its metabolites. Reproduced with permission from ref. 176. Copyright 2018, Elsevier. (C) Selective image of various pesticides detected by the paper-based sensor based on CdTe-nano ZnTPyP. Reproduced with permission from ref. 177. Copyright 2020, Elsevier. (D) Photograph and design showing the principle of the paper-based DNA biosensor. CZ: control area, TZ: experimental area. Reproduced with permission from ref. 179. Copyright 2020, Elsevier. (E) Calibration diagram of different doping contents (0–5%) in a binary mixture of bovine and goat yogurt samples. Reproduced with permission from ref. 179. Copyright 2020, Elsevier. (F) Paper-based electrical gas sensor manufacturing. Using a ballpoint pen and scissors, carbon electrodes were printed on Whatman chromatography 1# cellulose paper according to the desired shape and cut. Reproduced with permission from ref. 182. Copyright 2019, American Chemical Society. (G) Response of paper-based electrical gas sensors ( $n = 4$ ) to cod fillet decay at room temperature, compared with water ( $n = 2$ ) over 50 h. Reproduced with permission from ref. 182. Copyright 2019, American Chemical Society. (H) As a control ( $n = 2$ ), the paper-based electrical gas sensor ( $n = 4$ ) responded to cod fillet and water decay at 4 °C over 12 days. Reproduced with permission from ref. 182. Copyright 2019, American Chemical Society.

DNA from processed meat components. Mitochondrial genomic DNA is considered as a good candidate for reliable identification of meat components,<sup>179</sup> and from the adulteration rate of 0.1%, the authors successfully detected mitochondrial DNA from different meat samples with this device.

Freshness has a great influence on the nutritional value and taste of food, and eating spoiled food often causes some harm to consumers. Therefore, the development of food freshness detection devices is also extremely important in food production, and some researchers have developed paper-based sensors for food freshness detection. Tseng

et al.<sup>181</sup> fabricated a paper-based plasma refractive sensor by embedding metal nanoparticles on flexible paper using reverse nanoimprint lithography and used it to monitor the freshness of salmon foods. Barandun et al.<sup>182</sup> reported a new type of printed electrical gas sensor produced in a nearly “zero cost” manner (Fig. 10F). The sensors can be integrated into food packaging to monitor food freshness, reducing food waste and plastic pollution, or can be used as wireless, battery-free gas sensors in near-field communication labels via smart-phones. The sensor was based on the inherent moisture absorption of cellulose fibers in the paper; although paper looks dry, it actually contains a large amount of water

absorbed from the environment, so gases could be sensed by exploiting this factor rather than manually adding water to the substrate. The authors used this sensor to monitor the spoilage of meat products at room temperature nondestructively, and over the course of the experiment, the sensor response values increased by more than 900% in containers containing cod fillets compared to control experiments using DI water only (Fig. 10G). This increase was due to the release of gases from rotting meat. The authors also detected the spoilage gas of cod fillet at a low storage temperature of 4 °C (Fig. 10H). According to the detection results at room temperature, the product would no longer be safe to eat when stored at 4 °C for 4–5 days in the refrigerator, which was consistent with the advice issued by the manufacturer. Similarly, Mustafa *et al.*<sup>54</sup> reported a cost-effective enzyme-based paper-based biosensor, which could monitor fish freshness and predict spoilage. The biosensor used xanthine oxidase to convert xanthine to measure the release of hypoxanthine, a degradation index of meat and fish. This biosensor had high selectivity for hypoxanthine and was cheap and easy to manufacture. By tracking the degradation of fish with time and measuring the hypoxanthine concentration from 117 ( $\pm 9$ ) to 198 ( $\pm 5$ )  $\mu\text{M}$  within 24 hours after degradation, the applicability of the biosensor was proved, and its level was equivalent to that measured by commercial enzyme kits for hypoxanthine detection.

#### 4.4 Environmental monitoring

Environmental pollution and damage have come as a result of increased industrialization, and many factors such as waste gas and wastewater from factories, domestic sewage, automobile exhaust, pesticides and the constant use of chemical fertilizers contribute to the deterioration of water, air and soil quality.<sup>39</sup> Environmental problems not only render our living environment unsuitable for both humans and all kinds of plants and animals, but also impair health and wellbeing through constant pollution. Therefore, the detection of substances in the environment can help us to find problems quickly and carry out remedial measures. Paper-based devices provide simple, inexpensive and fast detection methods for substances in the environment, different from many traditional detection methods.<sup>39,183</sup>

The presence of appropriately low concentrations of metal ions in water is beneficial to humans, animals and plants. However, excessive amounts of metal ions can have negative effects.<sup>183</sup> Heavy metal ions, in particular, are highly toxic even at trace levels, and their contamination poses a huge threat to the environment and to public health around the world, potentially damaging ecosystems and detrimental to global sustainability.<sup>184,185</sup> These metals often exist as ions in aqueous solutions, and therefore researchers have developed paper-based detection sensors for detecting metal ions in water. Nie *et al.*<sup>186</sup> designed a paper-based microfluidic electrochemical sensing device. Microfluidic channels were

produced on the paper substrate by photolithography or wax printing, and screen printing of conductive inks, including carbon and Ag/AgCl, was used to form the electrodes of the device. The authors used this device to quantitatively detect the concentration of various analytes, such as heavy metal ions and glucose, in an aqueous solution. This low-cost analysis equipment could be used in areas such as underdeveloped areas, public health, and environmental monitoring. Feng *et al.*<sup>187</sup> constructed an array of paper-based devices based on fluorescence methods that can perform semi-quantitative detection of seven different heavy metal ions. (Fig. 11A). By comparing the color change of samples with the color change from solutions of known concentration, semi-quantification with a visual readout of ion concentration was achieved. Jarujamrus *et al.*<sup>71</sup> produced barcode-based paper microfluidic analysis equipment to detect magnesium ions in wastewater (Fig. 11B). The device used rubber latex as a hydrophobic material to construct a microfluidic channel on the paper base. By covering different detection lines with EDTA solutions of different Mg(II) concentrations, significantly different bands could be generated after exposure of the detection device to different concentrations. Xiao *et al.*<sup>188</sup> developed an enhanced 3D paper-based device that could be combined with a personal glucose meter for high sensitivity and portable detection of Ag<sup>+</sup> (Fig. 11C and D). Ag<sup>+</sup> in the sample solution was loaded in the nanopore film, and 3,3',5,5'-tetramethylbenzidine in the film reduced Ag<sup>+</sup> to form silver nanoparticles. These nanoparticles could grow through subsequent reactions, leading to the blockage of some pores of the nanometer film. The fixed glucose was redissolved by the finite volume of solution through the nanopore membrane, and glucose was measured in the next layer using a personal glucose meter (Fig. 11C). The amount of glucose recorded was dependent on the Ag<sup>+</sup> level in the sample, and the sensor enabled simple, low-cost and low-concentration specific detection of analytes in artificial water samples as well as in real water samples from pond, tap, drinking and soil water in a matter of minutes.

There remain some issues with paper-based metal ion detection, and so researchers are focusing on solving these problems and improving detection performance. Sharifi *et al.*<sup>189</sup> developed a 3D origami-based sensor combined with PVC film, which solved the problem of uneven color in the detection area caused by the movement of the chromogenic reagent or dye leaching (Fig. 11E). In addition, a waste liquid layer was added to the sensor to load more analytes, thus increasing the detection limit. As a proof of concept, this sensor was used to detect Cu<sup>2+</sup>. To this end, pyrocatechol violet and chrome azure S were doped into PVC film as colorimetric agents and injected into the detection area. The sensor had good linearity in the range of 5.0–1400.0 and 5.0–200.0  $\text{mg L}^{-1}$ , and the detection limits in the presence of azo chromium and pyrocatechol violet are 1.7 and 1.9  $\text{mg L}^{-1}$ . Moniz *et al.*<sup>190</sup> developed a paper-based microfluidic device for the detection of Fe<sup>3+</sup> ions in water samples using ether-



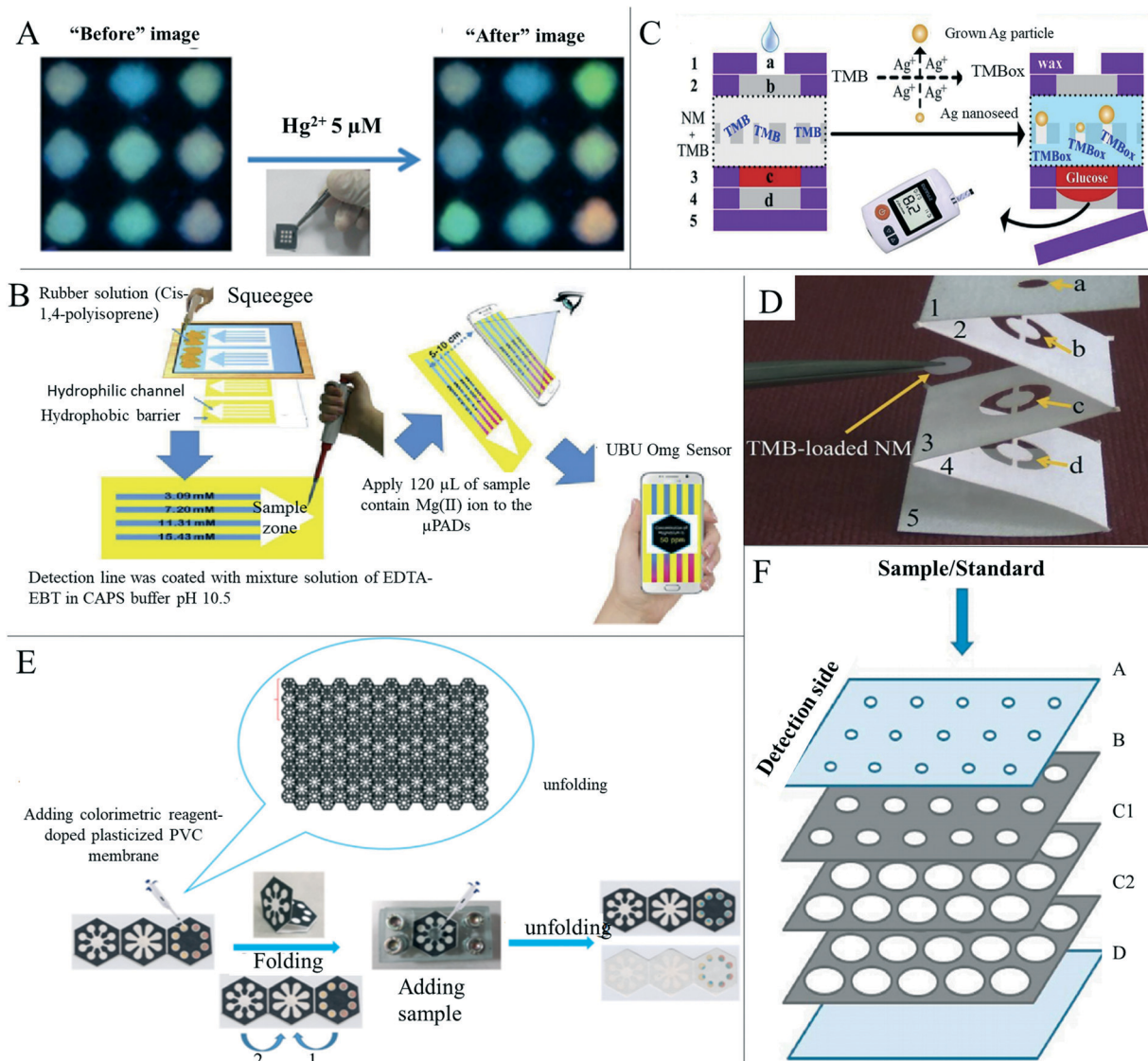


**Fig. 11** Paper-based sensors for metal ion detection in the environment. (A) Fluorescence identification of paper-based heavy metal ion sensor arrays before and after exposure to  $5 \mu M Hg^{2+}$  ions. Reproduced with permission from ref. 187. Copyright 2013, Elsevier. (B) Preparation and detection process of paper-based microfluidic analysis apparatus for magnesium ion detection. Reproduced with permission from ref. 71. Copyright 2019, Elsevier. (C) The paper-based enhanced biosensor to measure  $Ag^{+}$  concentrations, where the results were read quantitatively through a portable personal glucose meter. The paper-based device has five folding layers (numbered from 1 to 5). Functional area a of layer 1 is a 3.5 mm diameter circular well for sample addition. A 5 mm diameter circular functional area b from layer 2 was used for sample homogenization. Circular 5 mm diameter areas c and d located in the 3rd and 4th layers were used for glucose fixation and collection, respectively. Layer 5 is completely hydrophobic treated as the lowest layer of the device. Reproduced with permission from ref. 188. Copyright 2019, Elsevier. (D) 3D origami nanoporous membrane integrated microfluidic device. Reproduced with permission from ref. 188. Copyright 2019, Elsevier. (E) Process of design and application of the 3D folding analysis device for  $Cu^{2+}$  determination in water samples combined with PVC film. Reproduced with permission from ref. 189. Copyright 2020, Elsevier. (F) Schematic diagram of a newly developed paper-based microfluidic device for the determination of  $Fe^{3+}$  in natural waters. Layer A is the top layer of the device with pre-cut sample introduction holes. Layer B consists of 15 circular hydrophilic sample/assay regions (6 mm in diameter) each impregnated with 3-hydroxy-4-pyridine (3,4-HPO) reagent. C1 and C2 layers contain 15 pairs of circular hydrophilic sample storage areas with a diameter of 11 mm, which can accommodate standards/samples passing through the sample/detection areas. Layer D is the bottom layer of the device. Reproduced with permission from ref. 190. Copyright 2020, Elsevier.

derived 3-hydroxy-4-pyridinone chelators as color developing agents (Fig. 11F). The detection limit of the device was improved by using this new color reagent, and the detection signal was stable for four hours and the device has a stable storage period of at least one month.

In addition, some researchers have developed paper-based sensors that can detect multiple metal ions at the same time,

allowing for more efficient detection of metal ions. Wang *et al.*<sup>105</sup> developed a 3D paper-based microfluidic device for colorimetric determination of selected heavy metals in water samples with good selectivity by stacking wax-patterned paper layers and double-sided tape (Fig. 12A). The device could be used for detecting  $Cu^{(II)}$ ,  $Ni^{(II)}$ ,  $Cd^{(II)}$  and  $Cr^{(VI)}$  with detection limits of 0.29 ppm, 0.33 ppm, 0.19 ppm and 0.35 ppm,

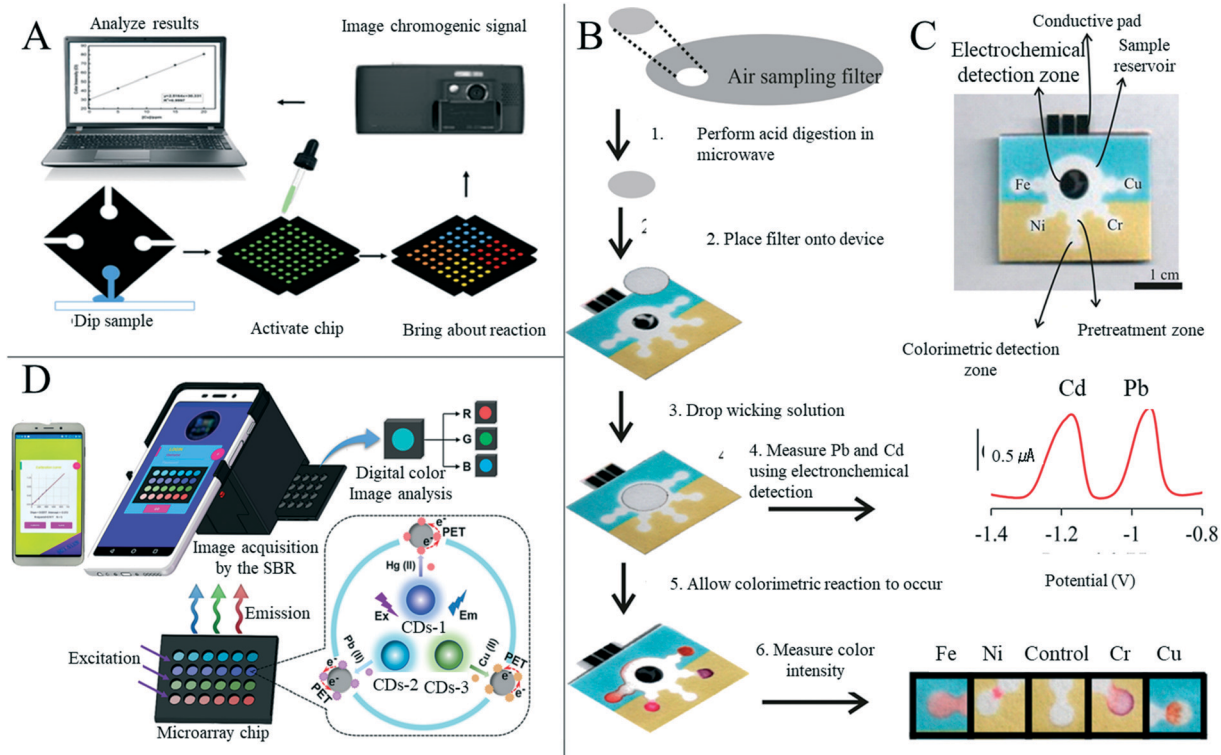


**Fig. 12** Paper-based sensors for simultaneous detection of multiple metal ions. (A) Schematic diagram of metal analysis based on three-dimensional paper microfluidics. The color signals were collected by a mobile phone camera and the data were analyzed by image processing and analysis software. Adapted with permission from ref. 105. Copyright 2014, Springer Nature. (B) An analytical procedure for performing metal analysis. The method requires three steps: (i) microwave-assisted acid digestion, (ii) anodic stripping volt-ampoule detection of Pb and Cd, and (iii) colorimetric detection of Fe, Ni, Cr and Cu. Adapted with permission from ref. 191. Copyright 2014, American Chemical Society. (C) Photographs of a multilayer paper-based microfluidic metal colorimetric and electrochemical analysis apparatus, with different areas labelled. Adapted with permission from ref. 191. Copyright 2014, American Chemical Society. (D) Sensors based on fluorescent carbon nanodots (CDs) were prepared on filter paper for simultaneous detection of various metal ions. Based on a smart phone portable reader and installing a customized APP, the fluorescence changes of sensors can be obtained and the results can be automatically reported. Adapted with permission from ref. 192. Copyright 2020, American Chemical Society.

respectively. The use of portable detectors and cellphones in combination with the device by the authors makes this 3D paper-based microfluidic device a simple, fast and on-site screening method for heavy metals in aquatic environments. A paper-based microfluidic device combining colorimetric and electrochemical detection into a three-dimensional structure was reported (Fig. 12B and C).<sup>191</sup> Different from previous detection devices, one layer of the device is used for colorimetric detection and the other layer is used for electrochemical detection. Different chemicals are simultaneously used in each layer of the detection area to detect the same sample, achieving the purpose of detecting different metal ions (Fig. 12B). The authors performed colorimetric detection of nickel, iron, copper and chromium, and electrochemical detection of lead and cadmium. The detection limit of the colorimetric layer was as low as 0.12  $\mu$ g of Cr, while the detection limit of the electrochemical layer was as low as 0.25 ng of Cd and Pb. Idros *et al.*<sup>185</sup> reported a low-cost, paper-based microfluidic analysis device that can easily, portably and simultaneously monitor mercury, lead, chromium, nickel, copper, and iron ions. Triple indicators, ligands containing ions, or molecules are preinstalled in

specific areas of the paper base. When metal ions were added, colorimetric indicators caused visible color changes to the naked eye. Using digital imaging and color calibration techniques, the color characteristics of red, green and blue (RGB) three-dimensional space were quantitatively analyzed. Xiao *et al.*<sup>192</sup> reported the use of paper-based microarray sensors based on carbon nanodot fluorescence turn-off for analytical object identification. The authors installed a stand-alone smart-phone based portable reader with a custom APP so that fluorescence changes could be accurately and repeatedly captured from microarray chips, results could be automatically reported, and reports could be generated and shared wirelessly (Fig. 12D). The above sensor system could simultaneously detect  $Hg^{2+}$ ,  $Pb^{2+}$  and  $Cu^{2+}$  in the water sample of the Pearl River. The end user operation was limited to moving the sample into the microarray chip, inserting the chip into the SBR, and opening the SBR-APP to obtain the image after importing the sample for 5 minutes. With the exception of needing a smart-phone, sophisticated sample preprocessing and expensive equipment were not required. The reliability and simplicity of this versatile and cost-effective smart-phone based sensor system makes it ideal for



user and ecologically friendly demand point detection in resource-constrained environments.

With the development of the chemical medicine industry and the increasing use of pesticides, toxic and harmful substances or excessive drug components deposited or remaining in the environment could have a great negative impact on our health.<sup>177</sup> Some developers have developed paper-based devices to detect toxic and harmful residues other than metal ions in the environment. Yakoh *et al.*<sup>193</sup> prepared a simple and selective paper-based colorimetric sensor using nano-silver for the determination of contaminant chlorine ions in the environment (Fig. 13A). The analysis was based on  $\text{Cl}^-$  oxidation of silver nano-prisms (AgNPrs) into smaller silver nanospheres (AgNPss). In the absence of surface modification, when  $\text{Cl}^-$  was present, the unique color change from dark purple to red could be quickly observed by the naked eye within 5 minutes, and a more obvious color change occurred with the increase in concentration (Fig. 13B). Nguyen *et al.*<sup>194</sup> developed a disposable, highly accurate, highly selective and low-cost paper-based probe for detecting gaseous amine compounds through a combination of color changes with seven pH indicators. The probe was designed with seven rings, printed

in wax and colored with different pH indicators. The probe's color was analyzed and RGB values were extracted from images obtained using a homemade mobile app. Zhou *et al.*<sup>195</sup> developed a paper-based detection device for the rapid and sensitive detection of tetracycline residues in environmental water. Fluorescence excitation was carried out by an ultraviolet lamp, and images were captured by a smart phone for quantitative analysis. Arduini *et al.*<sup>196</sup> developed an electrochemical biosensor based on origami for the detection of pesticide residues in the environment (Fig. 13C). The purpose of the study was to detect the three substances namely *p*-oxo, 2,4-dichlorophenoxyacetic acid and atrazine through the inhibiting ability of organophosphorus insecticides, phenoxy phenolic herbicides and triazine herbicides on butyrylcholinesterase, alkaline phosphatase and tyrosinase. The corresponding amount can be obtained according to the degree of inhibition of enzyme activity, and good results were obtained by sampling a standard solution and river water. Chen *et al.*<sup>197</sup> have reportedly developed a paper-based sensor for the detection of oxalyl chloride in the environment. When the detection device was placed in the vapor atmosphere containing oxalyl chloride, it produced an intramolecular charge transfer effect and showed a

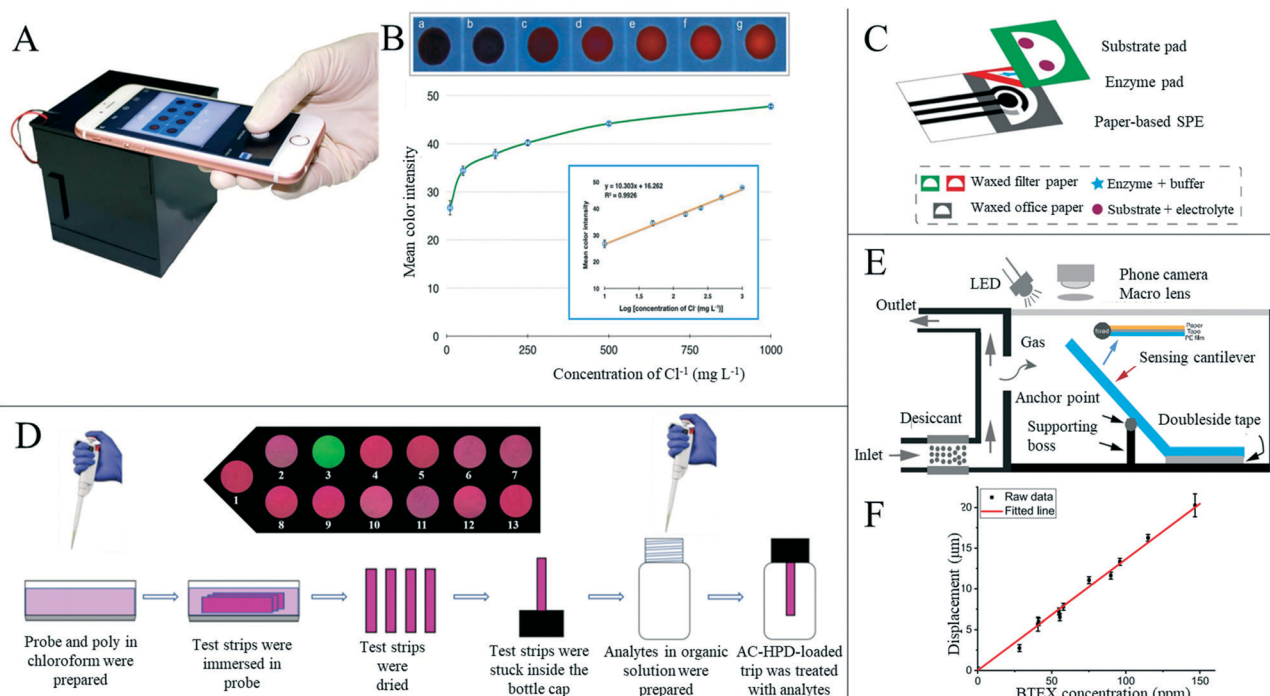


**Fig. 13** Paper-based sensors for detecting substances in the environment. (A) Photograph of  $\text{Cl}^-$  detection using a smart phone combined with a control box. Adapted with permission from ref. 193. Copyright 2018, Elsevier. (B) The visual images from paper sensors used to detect different  $\text{Cl}^-$  concentrations were analyzed using Image J software to determine the relationship between the average color intensity of AgNPrs and  $\text{Cl}^-$  concentration. Adapted with permission from ref. 193. Copyright 2018, Elsevier. (C) Image of the electrochemical biosensor for pesticide detection based on origami. Adapted with permission from ref. 196. Copyright 2019, Elsevier. (D) Schematic of a strip of paper-based sensor for the detection of chlorofluorocarbons. Insert is a 6 minute fluorescence photograph of oxalyl chloride, various nerve gas mimics and acyl chloride exposed to 120 ppm. Adapted with permission from ref. 197. Copyright 2020, Elsevier. (E) Fabrication and experimental setup of a sensing microcantilever. A cantilever beam is installed at the design position of the sensor chamber. The cantilever forms an inclination angle of  $45^\circ$  on the designed supporting platform. Adapted with permission from ref. 3. Copyright 2020, American Chemical Society. (F) Good linear relationship between BTEX concentration and microcantilever displacement. Sensitivity of the sensor is  $0.134 (\pm 0.0027) \mu\text{m ppm}^{-1}$ . Adapted with permission from ref. 3. Copyright 2020, American Chemical Society.



significant color change and fluorescence effect on oxalyl chloride (Fig. 13D). The device had a high reaction speed, high specificity, detection limit and obvious color and fluorescence change. Qin *et al.*<sup>3</sup> developed a simple, low-cost, light hydrocarbon gas sensor based on the principle of the bending of a paper-based cantilever caused by polymer swelling, and a smart-phone camera was used for data reading (Fig. 13E). The sensory cantilever consisted of three layers: the functional layer of polyethylene film, the adhesive layer of double-sided adhesive tape and the weighing paper substrate. The performance of the sensor was studied by using the hydrocarbons xylene, *n*-hexane and BTEX. The sensor showed good linear response to hydrocarbon concentration, a wide detection range, low detection, and fast response performance (Fig. 13F).

At present, some progress has been made in the research on paper-based sensors applied to environmental detection. A single device can analyze multiple substances simultaneously, which can greatly improve the detection efficiency. In addition, different detection methods have been developed, and multiple methods can be integrated on a single device, thus improving the accuracy of detection of the substance. Some issues still remain; currently, most devices are still in the laboratory stage of development and have not yet been mass-marketed. In addition, although many methods have been adopted to improve the accuracy of detection, there are still some deficiencies. When looking at samples from the field, most researchers have collected samples of lake water, river water and tap water, while there are few studies on the detection of substances in seawater, which accounts for the largest proportion.

## 5. Conclusions and future trends

In this review, we have discussed the manufacture of paper-based sensors and their applications in disease diagnosis, food safety, environmental protection and human behavior information detection. Significant progress has been made in manufacturing various paper-based sensors in many ways. In addition to wax printing, screen printing, laser treatment and plasma treatment with high precision, researchers have developed a series of preparation methods, such as folding, adhesion, manual drawing or cutting, greatly promoting the paper-based sensor to enter the mature market. For disease diagnosis, a variety of detection methods have been developed and the kinds of detectable diseases are gradually increasing. A single device can perform simultaneous analysis of different markers of the same disease or simultaneous detection using different methods to achieve reliable results and can also perform simultaneous detection of multiple diseases to improve the detection efficiency. Functional nanomaterials or other modifications can improve the sensitivity of paper-based detection, laying a good foundation for further practical applications. In human physiological signal detection, sensors have gradually developed from a single signal detection sensor to an

integrated sensor that can detect multiple signals. Using devices such as paper-based friction nano-generators, we can also collect the waste energy from human movement when detecting related signals.

Paper-based signal analysis has a long history, but development has been slow. Since the Whitesides group put forward the concept of paper-based microfluidics, however, research on paper-based analysis and testing has begun to explode. Compared with previous paper-based chemical testing, paper-based microfluidic devices achieve better fluid flow specification and higher signal detection. In addition, the continuous development and maturation of fabrication techniques has made it possible to fabricate paper-based devices on a large scale. It is increasingly recognized that worldwide use of low-cost paper-based rapid detection is necessary. Since the COVID-19 pandemic in particular, there has been a growing recognition of the importance of making a broad and rapid diagnosis. The above reasons have prompted the explosive growth of the research on paper-based detection. Some mature paper-based sensor products have already been applied in the market, such as the implementation of rapid influenza A<sup>+</sup> influenza B detection, the clearview 1 malaria prediction test and the RAIDTM 5 multi-lateral flow analysis detection device for determining biological threat factors.<sup>118</sup> However, although paper-based sensors are constantly being innovated, there is still a long way to go for mass market-oriented and mature applications of paper-based sensors.

The most important and obvious advantages of paper-based sensors lie in the inherent properties of paper, such as low cost, bio-compatibility and easy degradation. The significance of paper-based sensor research is to provide convenience for people's lives in the future, including health, food safety and environmental protection, while taking into account the existing conditions in remote and underdeveloped areas. Therefore, the most important factors that should be considered when developing these sensors include using a simple, uncomplicated manufacturing process and the ability for someone with little-to-no training to easily use and read results from this technology: this is essential for paper-based sensors to enter the market. We also think that for the marketization and mass production of paper-based sensors to occur, the following challenges and problems must be addressed: i) sensors made in different production batches must have repeatable detection performance within an allowable error range. ii) Different detection environments may affect test results. At present, most paper-based sensors are used to carry out various tests in a laboratory environment. A mature paper-based product must target people in different regions, and so we have to consider the impact of environmental changes on the test results. iii) The main development goal of low-cost paper-based detection devices is to realize point-of-care testing of diseases in underdeveloped areas. Therefore, the production cost of paper-based devices is also a problem that must be faced. Although the cost is currently low for preparing paper-



based devices in the laboratory, the actual mass production often needs to face various complicated economic expenditures. For example, manufacturers face multiple economic expenses, such as leasing space, purchasing instruments, paying technicians and R&D personnel, which may lead to higher costs for the final devices.

The continuous in-depth and detailed research on paper-based sensors has played a positive role in promoting their future maturity and marketization. For example, researchers have used tattooed paper as a substrate to prepare paper-based sensors to realize long-term, real-time detection of food and analysis of eating conditions, or combined with drugs to realize *in vivo* drug analysis and detection.<sup>198</sup> Paper-based sensors are still in the initial stage of development, and a large number of in-depth and continuous studies are required to move from laboratory research to practical application. Simultaneously, there are challenges such as the durability and stretch-ability of paper, the versatility of devices, and mass production requirements. When paper-based sensors are applied to certain specific scenarios, some advantages will become disadvantages. For example, because of its porous microstructure, paper has poor water resistance and low barrier property, and cannot maintain proper functionality when it encounters water or is stored in a high relative humidity environment.<sup>199</sup> In addition, the tensile property of paper is poor, limiting its use as a tensile sensor, and the size of holes between paper fibers is uncertain, potentially affecting the performance of devices such as microfluidics.<sup>200</sup> Some researchers have been working to solve the above problems, and for example, paper-based sensors with hydrophobic properties have made some progress.<sup>201</sup> Paper-based detection devices are also required to accurately identify the target analyte and provide readable signals, such as optical or electrical signals. These detection signals depend on the solubility of the target analyte, the nature of the signal-enhancing nanomaterials selected, and their specific binding. Different from the standard solution configured in the laboratory, the actual patient sample is complicated and contains many factors that interfere with the accurate reading of results. As in paper-based immunoassays, antibodies, proteins, peptides, and nucleic acids as target analytes may show cross-reactivity to similar biomarkers.<sup>202</sup> This will lead to false positives of the target diseases that we are testing. In addition, the fluorescence signal detected by the paper-based fluorescence sensor was sensitive to both internal and external conditions, such as pH and the solvating environment of the dye.<sup>202</sup> Paper-based detection also depends more on the capillary action of paper, and there are concerns about whether capillary action will affect the detection results as the concentration of the target substance in the sample may change due to adsorption onto the paper when the sample flows through the paper-based microfluidic channel. It should also be appreciated that the analytical materials used in the paper-based sensor (*e.g.*, specific antibodies and serum proteins) typically need to be stored at low temperature and for a short time. Furthermore,

the process of synthesizing antibodies that recognize the analyte of interest is challenging because the toxicity of the analyte injected into an animal may not be tolerated by the animal.<sup>203</sup> Therefore, the development of non-toxic and thermally stable analytical reagents is another research target of paper-based sensors.<sup>109</sup>

At present, we are gradually entering the 5G era, and the Internet has penetrated every aspect of our day-to-day lives. Combining new sensor technologies with the internet will be the main development direction for paper-based sensors in the future. For example, through the combination with smart phones, the detection results of the paper-based sensors could be uploaded to a personal database for simple real-time analysis and alerts, and the detection results could also be sent to relevant personnel for analysis of results.<sup>204</sup> This would provide convenience for people and alleviate the imbalance of medical resources, food analysis, environmental testing and other conditions in underdeveloped regions.

When using paper-based sensors for detection, a certain amount of energy is usually required, but at present, it is mostly realized by external connection. The energy supply problem of paper-based sensors is also a challenge in their current development, as they should still meet the requirements of flexibility, portability and wearability. Some researchers put forward the idea of a paper-based microfluidic battery, which could also provide a certain amount of energy when using microfluidic technology for detection. In addition, it could also collect the mechanical energy generated during the movement of the human body to realize the self-energy supply of the paper-based sensing device. The combination with NFC technology is also a popular development direction for both a wireless power supply and data transmission for paper-based sensors in the future. At present, although paper-based sensing technology utilizing NFC is still in its initial stage, the potential NFC brings makes sensing concepts such as no requirement for external power and integrated wireless data transmission possible, which may play an important role in the future revolution of interconnected technology.<sup>205</sup> We believe that the paper-based sensor in the future should be able to detect much information, such as human health and food safety, in real time and collect waste energy simultaneously, following the direction of many researchers' efforts at present.

## Conflicts of interest

The authors declare no competing financial interest.

## Acknowledgements

This work was financially supported by the National Key R&D Program of China (2017YFA0204700), the Joint Research Funds of Department of Science & Technology of Shaanxi Province and Northwestern Polytechnical University (No. 2020GXLY-Z-021), and Fundamental Research Funds for the Central Universities. FG and PC thank EPSRC Centre for



Doctoral Training in Plastic Electronics (EP/L016702/1) for the financial support. FG and PC also thank Imperial College Centre for Processable Electronics and Department of Bioengineering.

## References

- 1 C. Dincer, R. Bruch, E. Costa-Rama, M. T. Fernández-Abedul, A. Merkoçi, A. Manz, G. A. Urban and F. Güder, *Adv. Mater.*, 2019, **31**, 1806739.
- 2 A. W. Martinez, S. T. Phillips, G. M. Whitesides and E. Carrilho, *Anal. Chem.*, 2010, **82**, 3–10.
- 3 X. Qin, T. Wu, Y. Zhu, X. Shan, C. Liu and N. Tao, *Anal. Chem.*, 2020, **92**, 8480–8486.
- 4 K. Tenda, B. van Gerven, R. Arts, Y. Hiruta, M. Merkx and D. Citterio, *Angew. Chem., Int. Ed.*, 2018, **57**, 15369–15373.
- 5 J. P. Comer, *Anal. Chem.*, 1956, **28**, 1748–1750.
- 6 A. W. Martinez, S. T. Phillips, M. J. Butte and G. M. Whitesides, *Angew. Chem., Int. Ed.*, 2007, **46**, 1318–1320.
- 7 D. D. Liana, B. Raguse, J. J. Gooding and E. Chow, *Sensors*, 2012, **12**, 11505–11526.
- 8 C. Liu, F. A. Gomez, Y. Miao, P. Cui and W. Lee, *Talanta*, 2019, **194**, 171–176.
- 9 Q. H. Nguyen and M. I. Kim, *TrAC, Trends Anal. Chem.*, 2020, **132**, 116038.
- 10 L. L. Shen, G. R. Zhang and B. J. M. Etzold, *ChemElectroChem*, 2019, **7**, 10–30.
- 11 L. Gao, C. Zhu, L. Li, C. Zhang, J. Liu, H. D. Yu and W. Huang, *ACS Appl. Mater. Interfaces*, 2019, **11**, 25034–25042.
- 12 A. C. Glavan, R. V. Martinez, A. B. Subramaniam, H. J. Yoon, R. M. D. Nunes, H. Lange, M. M. Thuo and G. M. Whitesides, *Adv. Funct. Mater.*, 2014, **24**, 60–70.
- 13 L. Zong, Y. Han, L. Gao, C. Du, X. Zhang, L. Li, X. Huang, J. Liu, H. D. Yu and W. Huang, *Analyst*, 2019, **144**, 7157–7161.
- 14 X. Tao, H. Jia, Y. He, S. Liao and Y. Wang, *ACS Sens.*, 2017, **2**, 449–454.
- 15 M. Santhiago, P. G. da Costa, M. P. Pereira, C. C. Correa, V. B. de Moraes and C. C. B. Bufon, *ACS Appl. Mater. Interfaces*, 2018, **10**, 35631–35638.
- 16 H. Tai, Z. Duan, Y. Wang, S. Wang and Y. Jiang, *ACS Appl. Mater. Interfaces*, 2020, **12**, 31037–31053.
- 17 S. S. Das, S. Kar, T. Anwar, P. Saha and S. Chakraborty, *Lab Chip*, 2018, **18**, 1560–1568.
- 18 L. L. Shen, G. R. Zhang, M. Biesalski and B. J. M. Etzold, *Lab Chip*, 2019, **19**, 3438–3447.
- 19 X. He, Y. Zi, H. Yu, S. L. Zhang, J. Wang, W. Ding, H. Zou, W. Zhang, C. Lu and Z. L. Wang, *Nano Energy*, 2017, **39**, 328–336.
- 20 P.-K. Yang, Z.-H. Lin, K. C. Pradel, L. Lin, X. Li, X. Wen, J.-H. He and Z. L. Wang, *ACS Nano*, 2015, **9**, 901–907.
- 21 X. Gao, L. Huang, B. Wang, D. Xu, J. Zhong, Z. Hu, L. Zhang and J. Zhou, *ACS Appl. Mater. Interfaces*, 2016, **8**, 35587–35592.
- 22 X. Fan, J. Chen, J. Yang, P. Bai, Z. Li and Z. L. Wang, *ACS Nano*, 2015, **9**, 4236–4243.
- 23 R. Guo, J. Chen, B. Yang, L. Liu, L. Su, B. Shen and X. Yan, *Adv. Funct. Mater.*, 2017, **27**, 1702394.
- 24 C. Ma, W.-T. Cao, W. Xin, J. Bian and M.-G. Ma, *Ind. Eng. Chem. Res.*, 2019, **58**, 12018–12027.
- 25 S. W. Kang and J. Bae, *Macromol. Res.*, 2018, **26**, 226–232.
- 26 Y. Lv, F. Gong, H. Li, Q. Zhou, X. Wu, W. Wang and R. Xiao, *Appl. Energy*, 2020, **279**, 115764.
- 27 L. Zong, Y. Han, L. Gao, C. Du, X. Zhang, L. Li, X. Huang, J. Liu, H. D. Yu and W. Huang, *Analyst*, 2019, **144**, 7157–7161.
- 28 Y. Zhang, L. Zhang, K. Cui, S. Ge, X. Cheng, M. Yan, J. Yu and H. Liu, *Adv. Mater.*, 2018, **30**, e1801588.
- 29 Y. Lin, D. Gritsenko, Q. Liu, X. Lu and J. Xu, *ACS Appl. Mater. Interfaces*, 2016, **8**, 20501–20515.
- 30 B. Yao, J. Zhang, T. Kou, Y. Song, T. Liu and Y. Li, *Adv. Sci.*, 2017, **4**, 1700107.
- 31 E. Armstrong, *Nature*, 1931, **128**, 949–950.
- 32 S. M. Khan, J. M. Nassar and M. M. Hussain, *ACS Appl. Electron. Mater.*, 2020, **3**, 30–52.
- 33 D. Tobjörk and R. Österbacka, *Adv. Mater.*, 2011, **23**, 1935–1961.
- 34 M. M. Gong and D. Sinton, *Chem. Rev.*, 2017, **117**, 8447–8480.
- 35 E. Noviana, D. B. Carrão, R. Pratiwi and C. S. Henry, *Anal. Chim. Acta*, 2020, **1116**, 70–90.
- 36 K. Mao, X. Min, H. Zhang, K. Zhang, H. Cao, Y. Guo and Z. Yang, *J. Controlled Release*, 2020, **322**, 187–199.
- 37 W. K. T. Coltro, D. P. de Jesus, J. A. F. da Silva, C. L. do Lago and E. Carrilho, *Electrophoresis*, 2010, **31**, 2487–2498.
- 38 A. W. Martinez, *Bioanalysis*, 2011, **3**, 2589–2592.
- 39 C.-T. Kung, C.-Y. Hou, Y.-N. Wang and L.-M. Fu, *Sens. Actuators, B*, 2019, **301**, 126855.
- 40 A. Rayaprolu, S. K. Srivastava, K. Anand, L. Bhati, A. Asthana and C. M. Rao, *Anal. Chim. Acta*, 2018, **1044**, 86–92.
- 41 E. W. Nery and L. T. Kubota, *Anal. Bioanal. Chem.*, 2013, **405**, 7573–7595.
- 42 R. Tang, M. Y. Xie, M. Li, L. Cao, S. Feng, Z. Li and F. Xu, *Appl. Mater. Today*, 2022, **26**, 101305.
- 43 Y. Lu, W. Shi, J. Qin and B. Lin, *Anal. Chem.*, 2010, **82**, 329–335.
- 44 Q. Jiang, T. Han, H. Ren, A. U. R. Aziz, N. Li, H. Zhang, Z. Zhang and B. Liu, *Electrophoresis*, 2020, **41**, 1509–1516.
- 45 J. Jin, D. Lee, H. G. Im, Y. C. Han, E. G. Jeong, M. Rolandi, K. C. Choi and B. S. Bae, *Adv. Mater.*, 2016, **28**, 5169–5175.
- 46 H. Zhu, Z. Fang, C. Preston, Y. Li and L. Hu, *Energy Environ. Sci.*, 2014, **7**, 269–287.
- 47 M. Nogi, S. Iwamoto, A. N. Nakagaito and H. Yano, *Adv. Mater.*, 2009, **21**, 1595–1598.
- 48 N. Isobe, T. Kasuga and M. Nogi, *RSC Adv.*, 2018, **8**, 1833–1837.
- 49 J. W. Zhong, H. L. Zhu, Q. Z. Zhong, J. Q. Dai, W. B. Li, S. H. Jang, Y. G. Yao, D. Henderson, Q. Y. Hu, L. B. Hu and J. Zhou, *ACS Nano*, 2015, **9**, 7399–7406.
- 50 B. Ying, S. Park, L. Chen, X. Dong, E. W. K. Young and X. Liu, *Lab Chip*, 2020, **20**, 3322–3333.
- 51 G. Dinesh and B. Kandasubramanian, *Mater. Chem. Phys.*, 2022, **281**, 125707.
- 52 A. C. Glavan, D. C. Christodouleas, B. Mosadegh, H. D. Yu, B. S. Smith, J. Lessing, M. T. Fernández-Abedul and G. M. Whitesides, *Anal. Chem.*, 2014, **86**, 11999–12007.



53 X. Guo, L. Zong, Y. Jiao, Y. Han, X. Zhang, J. Xu, L. Li, C.-W. Zhang, Z. Liu, Q. Ju, J. Liu, Z. Xu, H. D. Yu and W. Huang, *Anal. Chem.*, 2019, **91**, 9300–9307.

54 F. Mustafa and S. Andreescu, *ACS Sens.*, 2020, **5**, 4092–4100.

55 Y. Jiao, C. Du, L. Zong, X. Guo, Y. Han, X. Zhang, L. Li, C. Zhang, Q. Ju, J. Liu, H. D. Yu and W. Huang, *Sens. Actuators, B*, 2020, **306**, 127239–127239.

56 J. Guo, W. Fang, A. Welle, W. Feng, I. Filpponen, O. J. Rojas and P. A. Levkin, *ACS Appl. Mater. Interfaces*, 2016, **8**, 34115–34122.

57 M. Zhu, C. Jia, Y. Wang, Z. Fang, J. Dai, L. Xu, D. Huang, J. Wu, Y. Li, J. Song, Y. Yao, E. Hitz, Y. Wang and L. Hu, *ACS Appl. Mater. Interfaces*, 2018, **10**, 28566–28571.

58 M. Zhu, Y. Wang, S. Zhu, L. Xu, C. Jia, J. Dai, J. Song, Y. Yao, Y. Wang, Y. Li, D. Henderson, W. Luo, H. Li, M. L. Minus, T. Li and L. Hu, *Adv. Mater.*, 2017, **29**, 1606284.

59 S. Sun, S. Feng, C. Ji, M. Shi, X. He, F. Xu and T. J. Lu, *J. Membr. Sci.*, 2020, **595**, 117502.

60 R. Tang, L. Liu, M. Li, X. Yao, Y. Yang, S. Zhang and F. Li, *Anal. Chem.*, 2020, **92**, 14219–14227.

61 D. A. Bruzewicz, M. Reches and G. M. Whitesides, *Anal. Chem.*, 2008, **80**, 3387–3392.

62 M. Baharfar, M. Rahbar, M. Tajik and G. Liu, *Biosens. Bioelectron.*, 2020, **167**, 112506.

63 M. Gutierrez-Capitan, A. Baldi and C. Fernandez-Sanchez, *Sensors*, 2020, **20**, 967.

64 A. Antonacci, V. Scognamiglio, V. Mazzaracchio, V. Caratelli, L. Fiore, D. Moscone and F. Arduini, *Front. Bioeng. Biotechnol.*, 2020, **8**, 339.

65 H. Koga, K. Nagashima, Y. Huang, G. Zhang, C. Wang, T. Takahashi, A. Inoue, H. Yan, M. Kanai, Y. He, K. Uetani, M. Nogi and T. Yanagida, *ACS Appl. Mater. Interfaces*, 2019, **11**, 15044–15050.

66 Y. Lu, W. Shi, L. Jiang, J. Qin and B. Lin, *Electrophoresis*, 2009, **30**, 1497–1500.

67 E. Carrilho, A. W. Martinez and G. M. Whitesides, *Anal. Chem.*, 2009, **81**, 7091–7095.

68 L. OuYang, C. Wang, F. Du, T. Zheng and H. Liang, *RSC Adv.*, 2014, **4**, 1093–1101.

69 Y. Sameenoi, P. N. Nongkai, S. Nouanthavong, C. S. Henry and D. Nacapricha, *Analyst*, 2014, **139**, 6580–6588.

70 W. Dungchai, O. Chailapakul and C. S. Henry, *Analyst*, 2011, **136**, 77–82.

71 P. Jarujamrus, R. Meelapsom, P. Nakken, N. Ditcharoen, W. Anutrasakda, A. Siripinyanond, M. Amatatongchai and S. Supasorn, *Anal. Chim. Acta*, 2019, **1082**, 66–77.

72 J. L. Delaney, C. F. Hogan, J. Tian and W. Shen, *Anal. Chem.*, 2011, **83**, 1300–1306.

73 M. Zhao, H. Li, W. Liu, Y. Guo and W. Chu, *Biosens. Bioelectron.*, 2016, **79**, 581–588.

74 C. Park, H.-R. Kim, S.-K. Kim, I.-K. Jeong, J.-C. Pyun and S. Park, *ACS Appl. Mater. Interfaces*, 2019, **11**, 36428–36434.

75 X. Li, J. F. Tian, T. Nguyen and W. Shen, *Anal. Chem.*, 2008, **80**, 9131–9134.

76 E. M. Fenton, M. R. Mascarenas, G. P. Lopez and S. S. Sibbett, *ACS Appl. Mater. Interfaces*, 2009, **1**, 124–129.

77 Y. Zhang, J. Liu, H. Wang and Y. Fan, *RSC Adv.*, 2019, **9**, 11460–11464.

78 M. M. Thuo, R. V. Martinez, W.-J. Lan, X. Liu, J. Barber, M. B. J. Atkinson, D. Bandarage, J.-F. Bloch and G. M. Whitesides, *Chem. Mater.*, 2014, **26**, 4230–4237.

79 Y. Guan, K. Zhang, F. Xu, R. Guo, A. Fang, B. Sun, X. Meng, Y. Liu and M. Bai, *Lab Chip*, 2020, **20**, 2724–2734.

80 M. Z. Hua and X. Lu, *ACS Sens.*, 2020, **5**, 4048–4056.

81 E. B. Strong, S. A. Schultz, A. W. Martinez and N. W. Martinez, *Sci. Rep.*, 2019, **9**, 7.

82 J. S. Ng and M. Hashimoto, *RSC Adv.*, 2020, **10**, 29797–29807.

83 C. K. Chiang, A. Kurniawan, C. Y. Kao and M. J. Wang, *Talanta*, 2019, **194**, 837–845.

84 S. Altundemir, A. K. Uguz and K. Ulgen, *Biomicrofluidics*, 2017, **11**, 041501.

85 S. Cinti, D. Talarico, G. Palleschi, D. Moscone and F. Arduini, *Anal. Chim. Acta*, 2016, **919**, 78–84.

86 V. Caratelli, A. Ciampaglia, J. Guiducci, G. Sancesario, D. Moscone and F. Arduini, *Biosens. Bioelectron.*, 2020, **165**, 112411.

87 M. A. Mahmud, E. J. M. Blondef, M. Kaddoura and B. D. MacDonald, *Analyst*, 2016, **141**, 6449–6454.

88 D. H. Hiep, Y. Tanaka, H. Matsubara and S. Ishizaka, *Anal. Sci.*, 2020, **36**, 1275–1278.

89 A. Kugimiya, A. Fujikawa, X. Jiang, Z. H. Fan, T. Nishida, J. Kohda, Y. Nakano and Y. Takano, *Appl. Biochem. Biotechnol.*, 2020, **192**, 812–821.

90 J. G. Giuliani, T. E. Benavidez, G. M. Duran, E. Vinogradova, A. Rios and C. D. Garcia, *J. Electroanal. Chem.*, 2016, **765**, 8–15.

91 G. M. Duran, T. E. Benavidez, J. G. Giuliani, A. Rios and C. D. Garcia, *Sens. Actuators, B*, 2016, **227**, 626–633.

92 W. R. de Araujo, C. M. R. Frasson, W. A. Ameku, J. R. Silva, L. Angnes and T. Paixao, *Angew. Chem., Int. Ed.*, 2017, **56**, 15113–15117.

93 C. Y. N. Nicoliche, A. M. Pascon, I. R. S. Bezerra, A. C. H. de Castro, G. R. Martos, J. Bettini, W. A. Alves, M. Santhiago and R. S. Lima, *ACS Appl. Mater. Interfaces*, 2022, **14**, 2522–2533.

94 F. M. Shimizu, A. M. Pasqualetti, C. Y. N. Nicoliche, A. L. Gobbi, M. Santhiago and R. S. Lima, *ACS Sens.*, 2021, **6**, 3125–3132.

95 S. Damasceno, C. C. Corrêa, R. F. Gouveia, M. Strauss, C. C. B. Bufon and M. Santhiago, *Adv. Electron. Mater.*, 2020, **6**, 1900826.

96 J. Olkkonen, K. Lehtinen and T. Erho, *Anal. Chem.*, 2010, **82**, 10246–10250.

97 S. Oyola-Reynoso, A. P. Heim, J. Halbertsma-Black, C. Zhao, I. D. Tevis, S. Çınar, R. Cademartiri, X. Liu, J.-F. Bloch and M. M. Thuo, *Talanta*, 2015, **145**, 73–77.

98 F. Ghaderinezhad, R. Amin, M. Temirel, B. Yenilmez, A. Wentworth and S. Tasoglu, *Sci. Rep.*, 2017, **7**, 3553.

99 M. Ponram, U. Balijapalli, B. Sambath, S. Kulathu Iyer, K. Kakaraparthi, G. Thota, V. Bakthavachalam, R. Cingaram, J. Sung-Ho and K. Natesan Sundaramurthy, *Dyes Pigm.*, 2019, **163**, 176–182.



100 C. Gaspar, J. Olkkonen, S. Passoja and M. Smolander, *Sensors*, 2017, **17**, 1464.

101 P. Sundriyal and S. Bhattacharya, *ACS Appl. Mater. Interfaces*, 2017, **9**, 38507–38521.

102 S. Liu, J. Li, X. Shi, E. Gao, Z. Xu, H. Tang, K. Tong, Q. Pei, J. Liang and Y. Chen, *Adv. Electron. Mater.*, 2017, **3**, 1700098.

103 P. J. He, I. N. Katis, R. W. Eason and C. L. Sones, *Lab Chip*, 2016, **16**, 3296–3303.

104 A. W. Martinez, S. T. Phillips and G. M. Whitesides, *Proc. Natl. Acad. Sci. U. S. A.*, 2008, **105**, 19606–19611.

105 H. Wang, Y.-j. Li, J.-f. Wei, J.-r. Xu, Y.-h. Wang and G.-x. Zheng, *Anal. Bioanal. Chem.*, 2014, **406**, 2799–2807.

106 J. Ding, B. Li, L. Chen and W. Qin, *Angew. Chem., Int. Ed.*, 2016, **55**, 13033–13037.

107 P. Teengam, W. Siangproh, A. Tuantranont, T. Vilaivan, O. Chailapakul and C. S. Henry, *Anal. Chem.*, 2017, **89**, 5428–5435.

108 H. Lim, A. T. Jafry and J. Lee, *Molecules*, 2019, **24**, 2869.

109 A. K. Yetisen, M. S. Akram and C. R. Lowe, *Lab Chip*, 2013, **13**, 2210–2251.

110 S.-G. Jeong, D.-H. Kim, J. Kim, J.-H. Kim, S. Song and C.-S. Lee, *Chem. Eng. J.*, 2021, **411**, 128429.

111 X. Li and X. Liu, *Microfluid. Nanofluid.*, 2014, **16**, 819–827.

112 K. Punpattanakul, S. Kraduangdej, N. Jiranusornkul, M. Chiaranairungroj, A. Pimpin, T. Palaga and W. Srituravanich, *Cellulose*, 2018, **25**, 2659–2665.

113 M. F. Mora, C. D. Garcia, F. Schaumburg, P. A. Kler, C. L. A. Berli, M. Hashimoto and E. Carrilho, *Anal. Chem.*, 2019, **91**, 8298–8303.

114 Y. Yang, E. Noviana, M. P. Nguyen, B. J. Geiss, D. S. Dandy and C. S. Henry, *Anal. Chem.*, 2016, **89**, 71–91.

115 H. Becker and C. Gärtner, in *Microchip Diagnostics*, 2017, ch. 1, pp. 3–21, DOI: 10.1007/978-1-4939-6734-6\_1.

116 M. Dou, S. T. Sanjay, M. Benhabib, F. Xu and X. Li, *Talanta*, 2015, **145**, 43–54.

117 Y. Xia, J. Si and Z. Li, *Biosens. Bioelectron.*, 2016, **77**, 774–789.

118 A. K. Yetisen, M. S. Akram and C. R. Lowe, *Lab Chip*, 2013, **13**, 2210.

119 G. Sriram, M. P. Bhat, P. Patil, U. T. Uthappa, H.-Y. Jung, T. Altalhi, T. Kumeria, T. M. Aminabhavi, R. K. Pai, Madhuprasad and M. D. Kurkuri, *TrAC, Trends Anal. Chem.*, 2017, **93**, 212–227.

120 S. S. Nadar, P. D. Patil, M. S. Tiwari and D. J. Ahirrao, *Crit. Rev. Biotechnol.*, 2021, **41**, 1046–1080.

121 J. Hu, S. Wang, L. Wang, F. Li, B. Pingguan-Murphy, T. J. Lu and F. Xu, *Biosens. Bioelectron.*, 2014, **54**, 585–597.

122 J. Songok and M. Toivakka, *ACS Appl. Mater. Interfaces*, 2016, **8**, 30523–30530.

123 S. Kim and H. D. Sikes, *ACS Appl. Mater. Interfaces*, 2019, **11**, 28469–28477.

124 C. Wang, X. Gao, S. Wang and Y. Liu, *Anal. Bioanal. Chem.*, 2020, **412**, 611–620.

125 G. G. Morbioli, T. Mazzu-Nascimento, A. M. Stockton and E. Carrilho, *Anal. Chim. Acta*, 2017, **970**, 1–22.

126 T.-T. Tsai, C.-Y. Huang, C.-A. Chen, S.-W. Shen, M.-C. Wang, C.-M. Cheng and C.-F. Chen, *ACS Sens.*, 2017, **2**, 1345–1354.

127 C.-A. Chen, P.-W. Wang, Y.-C. Yen, H.-L. Lin, Y.-C. Fan, S.-M. Wu and C.-F. Chen, *Sens. Actuators, B*, 2019, **282**, 251–258.

128 F. Li, X. Wang, J. Liu, Y. Hu and J. He, *Sens. Actuators, B*, 2019, **288**, 266–273.

129 K. Wang, J. Yang, H. Xu, B. Cao, Q. Qin, X. Liao, Y. Wo, Q. Jin and D. Cui, *Anal. Bioanal. Chem.*, 2020, **412**, 2517–2528.

130 P. Q. Nguyen, L. R. Soenksen, N. M. Donghia, N. M. Angenent-Mari, H. de Puig, A. Huang, R. Lee, S. Slomovic, T. Galbersanini, G. Lansberry, H. M. Sallum, E. M. Zhao, J. B. Niemi and J. J. Collins, *Nat. Biotechnol.*, 2021, **39**, 1366–1374.

131 M. Wu, Q. Lai, Q. Ju, L. Li, H. D. Yu and W. Huang, *Biosens. Bioelectron.*, 2018, **102**, 256–266.

132 L. Liang, M. Su, L. Li, F. Lan, G. Yang, S. Ge, J. Yu and X. Song, *Sens. Actuators, B*, 2016, **229**, 347–354.

133 X. Cai, H. Zhang, X. Yu and W. Wang, *Talanta*, 2020, **216**, 120996.

134 F. Bray, J. Ferlay, I. Soerjomataram, R. L. Siegel, L. A. Torre and A. Jemal, *Ca-Cancer J. Clin.*, 2018, **68**, 394–424.

135 I. Grabowska, N. Sharma, A. Vasilescu, M. Iancu, G. Badea, R. Boukherroub, S. Ogale and S. Szunerits, *ACS Omega*, 2018, **3**, 12010–12018.

136 W. Hu, Y. Liu, H. Yang, X. Zhou and C. M. Li, *Biosens. Bioelectron.*, 2011, **26**(8), 3683–3687.

137 S. Wang, L. Ge, X. Song, J. Yu, S. Ge, J. Huang and F. Zeng, *Biosens. Bioelectron.*, 2012, **31**, 212–218.

138 L. Zhang, Y. Hou, C. Lv, W. Liu, Z. Zhang and X. Peng, *Anal. Methods*, 2020, **12**, 4191–4198.

139 C. J. Valentine, K. Takagishi, S. Umezu, R. Daly and M. De Volder, *ACS Appl. Mater. Interfaces*, 2020, **12**, 30680–30685.

140 W. Dungchai, O. Chailapakul and C. S. Henry, *Anal. Chem.*, 2009, **81**, 5821–5826.

141 S. Cinti, R. Cusenza, D. Moscone and F. Arduini, *Talanta*, 2018, **187**, 59–64.

142 S. Boonkaew, P. Teengam, S. Jampasa, S. Rengpipat, W. Siangproh and O. Chailapakul, *Analyst*, 2020, **145**, 5019–5026.

143 M. Moccia, V. Caratelli, S. Cinti, B. Pede, C. Avitabile, M. M. Saviano, A. L. Imbriani, D. Moscone and F. Arduini, *Biosens. Bioelectron.*, 2020, **165**, 112371.

144 R. F. e. Silva, T. R. Longo Cesar Paixão, M. Der Torossian Torres and W. R. de Araujo, *Sens. Actuators, B*, 2020, **308**, 127669.

145 D. Maier, E. Laubender, A. Basavanna, S. Schumann, F. Guder, G. A. Urban and C. Dincer, *ACS Sens.*, 2019, **4**, 2945–2951.

146 T. Ming, J. Luo, J. Liu, S. Sun, Y. Xing, H. Wang, G. Xiao, Y. Deng, Y. Cheng, Z. Yang, H. Jin and X. Cai, *Biosens. Bioelectron.*, 2020, **170**, 112649.

147 Z. Nie, F. Deiss, X. Liu, O. Akbulut and G. M. Whitesides, *Lab Chip*, 2010, **10**, 3163–3169.

148 A. Nemirovski, D. C. Christodouleas, J. W. Hennek, A. A. Kumar, E. J. Maxwell, M. T. Fernandez-Abedul and G. M.



Whitesides, *Proc. Natl. Acad. Sci. U. S. A.*, 2014, **111**, 11984–11989.

149 J. Mettakoonpitak, K. Boehle, S. Nantaphol, P. Teengam, J. A. Adkins, M. Srisa-Art and C. S. Henry, *Electroanalysis*, 2016, **28**, 1420–1436.

150 H. C. Ates, A. K. Yetisen, F. Güder and C. Dincer, *Nat. Electron.*, 2021, **4**, 13–14.

151 L.-Q. Tao, K.-N. Zhang, H. Tian, Y. Liu, D.-Y. Wang, Y.-Q. Chen, Y. Yang and T.-L. Ren, *ACS Nano*, 2017, **11**, 8790–8795.

152 J. Zhang, G.-Y. Lee, C. Cerwyn, J. Yang, F. Fondjo, J.-H. Kim, M. Taya, D. Gao and J.-H. Chung, *Adv. Mater. Technol.*, 2018, **3**, 1700266.

153 T. Yang and J. M. Mativetsky, *ACS Appl. Mater. Interfaces*, 2019, **11**, 26339–26345.

154 C. Wang, X. Hou, M. Cui, J. Yu, X. Fan, J. Qian, J. He, W. Geng, J. Mu and X. Chou, *Sci. China Mater.*, 2019, **63**, 403–412.

155 Y. Long, P. He, R. Xu, T. Hayasaka, Z. Shao, J. Zhong and L. Lin, *Carbon*, 2020, **157**, 594–601.

156 Z. Han, H. Li, J. Xiao, H. Song, B. Li, S. Cai, Y. Chen, Y. Ma and X. Feng, *ACS Appl. Mater. Interfaces*, 2019, **11**, 33370–33379.

157 S. Li, Z. Ma, Z. Cao, L. Pan and Y. Shi, *Small*, 2019, **16**, 1903822.

158 H. C. Ates, A. Brunauer, F. Stetten, G. A. Urban, F. Güder, A. Merkoçi, S. M. Früh and C. Dincer, *Adv. Funct. Mater.*, 2021, **31**, 2010388.

159 M. Parrilla, T. Guinovart, J. Ferré, P. Blondeau and F. J. Andrade, *Adv. Healthcare Mater.*, 2019, **8**, 1900342.

160 H. Wu, L. Xu, Y. Wang, T. Zhang, H. Zhang, C. R. Bowen, Z. L. Wang and Y. Yang, *ACS Energy Lett.*, 2020, **5**, 3708–3717.

161 Y. Xu, G. Zhao, L. Zhu, Q. Fei, Z. Zhang, Z. Chen, F. An, Y. Chen, Y. Ling, P. Guo, S. Ding, G. Huang, P.-Y. Chen, Q. Cao and Z. Yan, *Proc. Natl. Acad. Sci. U. S. A.*, 2020, **117**, 18292–18301.

162 L. Ortega, A. Llorella, J. P. Esquivel and N. Sabaté, *Microsyst. Nanoeng.*, 2019, **5**, 3.

163 J. Luo, Y. Yao, X. Duan and T. Liu, *J. Mater. Chem. C*, 2018, **6**, 4727–4736.

164 H. Liu, H. Xiang, Y. Wang, Z. Li, L. Qian, P. Li, Y. Ma, H. Zhou and W. Huang, *ACS Appl. Mater. Interfaces*, 2019, **11**, 40613–40619.

165 S. Jo, I. Kim, N. Jayababu, H. Roh, Y. Kim and D. Kim, *ACS Sustainable Chem. Eng.*, 2020, **8**, 10786–10794.

166 K. Zhang, H. Li, W. Wang, J. Cao, N. Gan and H. Han, *ACS Sens.*, 2020, **5**, 3721–3738.

167 T. Ozer, C. McMahon and C. S. Henry, *Annu. Rev. Anal. Chem.*, 2020, **13**, 85–109.

168 K. Mahato and P. Chandra, *Biosens. Bioelectron.*, 2019, **128**, 9–16.

169 L. Zong, Y. Jiao, X. Guo, C. Zhu, L. Gao, Y. Han, L. Li, C. Zhang, Z. Liu, J. Liu, Q. Ju, H. D. Yu and W. Huang, *Talanta*, 2019, **195**, 333–338.

170 N. F. D. Silva, C. M. R. Almeida, J. M. C. S. Magalhães, M. P. Gonçalves, C. Freire and C. Delerue-Matos, *Biosens. Bioelectron.*, 2019, **141**, 111317.

171 K. Xia, Z. Zhu, H. Zhang, C. Du, J. Fu and Z. Xu, *Nano Energy*, 2019, **56**, 400–410.

172 X. Sha, S.-q.-g.-w. Han, H. Zhao, N. Li, C. Zhang and W.-L.-j. Hasi, *Anal. Sci.*, 2020, **36**, 667–674.

173 C. Zhou, H. Zou, M. Li, C. Sun, D. Ren and Y. Li, *Biosens. Bioelectron.*, 2018, **117**, 347–353.

174 F. P. Carvalho, *Food Energy Secur.*, 2017, **6**, 48–60.

175 L. Ma, A. Nilghaz, J. R. Choi, X. Liu and X. Lu, *Food Chem.*, 2018, **246**, 437–441.

176 Z. Wang, J. Zhang, L. Liu, X. Wu, H. Kuang, C. Xu and L. Xu, *Food Chem.*, 2019, **276**, 707–713.

177 H. Chen, O. Hu, Y. Fan, L. Xu, L. Zhang, W. Lan, Y. Hu, X. Xie, L. Ma, Y. She and H. Fu, *Food Chem.*, 2020, **327**, 127075.

178 E. Trofimchuk, Y. Hu, A. Nilghaz, M. Z. Hua, S. Sun and X. Lu, *Food Chem.*, 2020, **316**, 126396.

179 E. T. Bougadi and D. P. Kalogianni, *Food Chem.*, 2020, **322**, 126758.

180 B. S. Batule, Y. Seok and M.-G. Kim, *Food Chem.*, 2020, **321**, 126708.

181 S. Y. Tseng, S. Y. Li, S. Y. Yi, A. Y. Sun, D. Y. Gao and D. Wan, *ACS Appl. Mater. Interfaces*, 2017, **9**, 17306–17316.

182 G. Barandun, M. Soprani, S. Naficy, M. Grell, M. Kasimatis, K. L. Chiu, A. Ponzoni and F. Guder, *ACS Sens.*, 2019, **4**, 1662–1669.

183 N. A. Meredith, C. Quinn, D. M. Cate, T. H. Reilly, J. Volckens and C. S. Henry, *Analyst*, 2016, **141**, 1874–1887.

184 L.-L. Shen, G.-R. Zhang, W. Li, M. Biesalski and B. J. M. Etzold, *ACS Omega*, 2017, **2**(8), 4593–4603.

185 N. Idros and D. Chu, *ACS Sens.*, 2018, **3**, 1756–1764.

186 Z. Nie, C. A. Nijhuis, J. Gong, X. Chen, A. Kumachev, A. W. Martinez, M. Narovlyansky and G. M. Whitesides, *Lab Chip*, 2010, **10**, 477–483.

187 L. Feng, H. Li, L.-Y. Niu, Y.-S. Guan, C.-F. Duan, Y.-F. Guan, C.-H. Tung and Q.-Z. Yang, *Talanta*, 2013, **108**, 103–108.

188 W. Xiao, Y. Gao, Y. Zhang, J. Li, Z. Liu, J. Nie and J. Li, *Biosens. Bioelectron.*, 2019, **137**, 154–160.

189 H. Sharifi, J. Tashkhourian and B. Hemmateenejad, *Anal. Chim. Acta*, 2020, **1126**, 114–123.

190 T. Moniz, C. R. Bassett, M. I. G. S. Almeida, S. D. Kolev, M. Rangel and R. B. R. Mesquita, *Talanta*, 2020, **214**, 120887.

191 P. Rattanarat, W. Dungchai, D. Cate, J. Volckens, O. Chailapakul and C. S. Henry, *Anal. Chem.*, 2014, **86**, 3555–3562.

192 M. Xiao, Z. Liu, N. Xu, L. Jiang, M. Yang and C. Yi, *ACS Sens.*, 2020, **5**, 870–878.

193 A. Yakoh, P. Rattanarat, W. Siangproh and O. Chailapakul, *Talanta*, 2018, **178**, 134–140.

194 T.-T. T. Nguyen, B. T. Huy and Y.-I. Lee, *ACS Omega*, 2019, **4**, 12665–12670.

195 T. Zhou, J.-J. Liu, Y. Xu and Z.-Y. Wu, *Microchem. J.*, 2019, **145**, 703–707.



196 F. Arduini, S. Cinti, V. Caratelli, L. Amendola, G. Palleschi and D. Moscone, *Biosens. Bioelectron.*, 2019, **126**, 346–354.

197 T. Chen, L. Jiang, H.-Q. Yuan, Y. Zhang, D. Su and G.-M. Bao, *Sens. Actuators, B*, 2020, **319**, 128289.

198 G. E. Bonacchini, C. Bossio, F. Greco, V. Mattoli, Y.-H. Kim, G. Lanzani and M. Caironi, *Adv. Mater.*, 2018, **30**, 1706091.

199 K. Zeng, J. Gu and C. Cao, *ACS Appl. Mater. Interfaces*, 2020, **12**, 18987–18996.

200 W. C. Lee, H. Y. Ng, C. Y. Hou, C. T. Lee and L. M. Fu, *Lab Chip*, 2021, **21**, 1433–1453.

201 L. Liu, Z. Jiao, J. Zhang, Y. Wang, C. Zhang, X. Meng, X. Jiang, S. Niu, Z. Han and L. Ren, *ACS Appl. Mater. Interfaces*, 2021, **13**, 1967–1978.

202 D. R. Hristov, C. Rodriguez-Quijada, J. Gomez-Marquez and K. Hamad-Schifferli, *Sensors*, 2019, **19**, 554.

203 M. Sajid, A.-N. Kawde and M. Daud, *J. Saudi Chem. Soc.*, 2015, **19**, 689–705.

204 A. W. Martinez, S. T. Phillips, E. Carrilho, S. W. Thomas III, H. Sindi and G. M. Whitesides, *Anal. Chem.*, 2008, **80**, 3699–3707.

205 S. Olenik, H. S. Lee and F. Guder, *Nat. Rev. Mater.*, 2021, **6**, 286–288.

